

Shortcuts to adiabaticity for open quantum systems and a mixed-state inverse engineering scheme

S. L. Wu,^{1,*} W. Ma,¹ X. L. Huang,² and Xuexi Yi^{3,†}

¹*School of Physics and Materials Engineering, Dalian Nationalities University, Dalian 116600 China*

²*School of Physics and Electronic Technology, Liaoning Normal University, Dalian 116029, China*

³*Center for Quantum Sciences and School of Physics,
Northeast Normal University, Changchun 130024, China*

(Dated: January 5, 2022)

We propose a fast mixed-state control scheme to transfer the quantum state along designable trajectories in Hilbert space, which is robust to multiple decoherence noises. Starting with the dynamical invariants of open quantum systems, we present the shortcuts to adiabaticity (STAs) of open quantum systems at first, then apply the STAs to speed up the adiabatic steady process. Our scheme drives open systems from a initial steady state to a target steady state by a controlled Liouvillian that possesses the same form as the reference (original) one which is accessible in present-day experiments. The experimental observation with current available parameters for the nitrogen-vacancy (NV) center in diamond is suggested and discussed.

PACS numbers: 03.67.-a, 03.65.Yz, 05.70.Ln, 05.40.Ca

I. INTRODUCTION

Controlling quantum systems to accomplish special task is at the heart of emerging quantum technologies[1–3]. The ideal control scheme needs to satisfy three important issues: (i) High-speed: The quantum state transfers to the target state within desired control time length; (ii) High-fidelity: The control process should be with an admissible error; (iii) High-controllability: The trajectory from an initial state to a target state must be completely controllable.

The most selected schemes in experiment are based on the unitary evolution of closed systems[4–7]. Yet unwanted couplings to the environment reduce the fidelity severely[8, 9], and the final state can not be steadied on the target state after the control is done. This shackles the quantum sciences and technologies to realize efficient and scalable devices beyond the current circumstances of proof-of-principle demonstrations. To overcome such shackles, a straightforward thinking is to formulate a scheme based on the theory of open quantum systems. Due to its steadiness, the steady state becomes an important candidate to achieve the quantum control task[10]. The adiabatic steady state engineering scheme transfers the quantum state into the target state along instantaneous steady state[11, 12]. But the control process needs to be very slow so that the adiabatic condition can be satisfied. Also, the fast steady state engineering schemes are proposed to accelerate the adiabatic evolution of the equilibrium state of quantum thermodynamic system, which can only be applied to the Gibbs states or the Gaussian states [13, 14]. On the other hand, the transitionless quantum driving method of open quantum

systems is also proposed, but a feasible control protocol is hard to be presented[15, 16]. Therefore, up to present, none of schemes satisfies the requirements including high-accuracy, high-controllability, and high-speed at the same time.

In this paper, we propose a fast control scheme of open quantum systems, named the mixed-state inverse engineering scheme (MIE), which allows a robust and precise transfer to a given target state with a designable mixed state trajectory. Firstly, by analysing the spectral features of dynamical invariant superoperators of open quantum systems[17], we present general solutions of quantum states governed by the master equation

$$\partial_t |\rho(t)\rangle\rangle = \hat{\mathcal{L}}_c(t) |\rho(t)\rangle\rangle. \quad (1)$$

with the Liouvillian superoperator $\hat{\mathcal{L}}_c(t)$. Based on this general solution, the STAs of open quantum systems are established. Then, we apply the STAs of open quantum systems on the steady state engineering (i.e., the MIE scheme), and show that the target state can be reached with extremely high fidelity and within desired control time length. The central advantage of our scheme is that the control tasks are, in general, achieved with fruitful feasible control protocols in experiment by selecting different quantum state trajectories. More importantly, the selectable trajectories can bring the ideal final fidelity even multiple noise sources are involved. In fact, the pure-state inverse engineering scheme of closed quantum systems is a particular case of the STAs scheme of open quantum systems [18], when the trajectories of quantum states are the pure-state trajectories. And the MIE scheme can overcome the difficulties in the earlier STAs methods for closed system due to the designable mixed-state trajectory.

The rest of this paper is organized as follows. In Sec.II, we present the STAs scheme of open quantum systems, and propose the MIE scheme to accelerate the adiabatic steady state process. In Sec. III, we apply the

* slwu@dlnu.edu.cn

† yixx@nenu.edu.cn

MIE scheme to NV center system, which provides simple, practical, robust control protocols to transfer the population from one ground state to the other[19, 20]. It is shown that the MIE scheme is far better at transfer efficiency than any STAs scheme of closed systems[9], especially in the case that the three level system suffers from dissipation and dephasing at the same time. In Sec.IV, we discuss the relationship between the mixed-state inverse engineering scheme and the pure-state inverse engineering scheme of closed systems[18]. Conclusions are presented in Sec. V.

II. METHODS

A. STAs of Open Quantum Systems

For an open quantum system governed by Eq.(1), a dynamical invariant of the open quantum system is defined as a superoperator $\hat{\mathcal{I}}(t)$ which satisfies[17]

$$\partial_t \hat{\mathcal{I}}(t) - [\hat{\mathcal{L}}_c(t), \hat{\mathcal{I}}(t)] = 0. \quad (2)$$

In general, invariants are non-Hermitian. Thus $\hat{\mathcal{I}}(t)$ needs to be expressed as the Jordan canonical form. Consider that there are m Jordan blocks, and the α -th Jordan block is n_α -dimensional. According to the Jordan decomposition of $\hat{\mathcal{I}}(t)$, we introduce right vectors $\{|D_\alpha^{(i)}\rangle\}$ and left vectors $\{\langle E_\alpha^{(i)}|\}$ in the Hilbert-Schmidt space. The left and right vectors always satisfy

$$\begin{aligned} \hat{\mathcal{I}}|D_\alpha^{(i)}\rangle &= \lambda_\alpha|D_\alpha^{(i)}\rangle + |D_\alpha^{(i-1)}\rangle, \\ \langle E_\alpha^{(i)}|\hat{\mathcal{I}} &= \lambda_\alpha\langle E_\alpha^{(i)}| + \langle E_\alpha^{(i+1)}|, \end{aligned}$$

with $|D_\alpha^{(-1)}\rangle \equiv 0$, $\langle E_\alpha^{(n_\alpha)}| \equiv 0$ for $i = 0, 1, \dots, n_\alpha - 1$. Thus, the right and left vectors $|D_\alpha^{(0)}\rangle$ and $\langle E_\alpha^{(n_\alpha-1)}|$ are the right and left eigenstates of $\hat{\mathcal{I}}(t)$ with the eigenvalue λ_α . Here we assume that all of eigenvalues are nondegenerate, i.e., $\lambda_\alpha \neq \lambda_\beta$ for $\forall \alpha \neq \beta$. And the left and right vectors satisfy the orthonormality condition

$$\langle E_\alpha^{(i)}|D_\beta^{(j)}\rangle = \delta_{\alpha\beta}\delta_{ij}$$

It can be verified that the eigenvalues of the dynamical invariants are time-independent, and

$$\langle E_\beta^{(j)}|\hat{O}|D_\alpha^{(i)}\rangle = 0, \quad \forall i, j,$$

with $\hat{O} = \hat{\mathcal{L}} - \partial_t$ for $\alpha \neq \beta$. Therefore, it can be verified that the general solution of Eq.(1) reads

$$|\rho(t)\rangle = \sum_{\alpha=0}^{m-1} c_\alpha \exp(\eta_\alpha(t)) |\Phi_\alpha(t)\rangle, \quad (3)$$

in which $\eta_\alpha(t)$ is a complex phase, c_α is a time-independent expansion efficient. $|\Phi_\alpha(t)\rangle$ is a right vector in the α -th Jordan block, which can be written as

$$|\Phi_\alpha(t)\rangle = \sum_{i=0}^{n_\alpha-1} b_i^\alpha(t) |D_\alpha^{(i)}(t)\rangle, \quad (4)$$

with coefficients $b_i^\alpha(t)$. The details of the derivation of the general solution Eq.(3) can be found in Appendix. A.

Since the adiabaticity of open quantum systems requires only forbidding the transition between different Jordan blocks[10], the general solution Eq.(3) is enough to establish STAs of open quantum systems. Suppose that our aim is to drive the quantum system from an initial Liouvillian $\hat{\mathcal{L}}_c(0)$ to a final one $\hat{\mathcal{L}}_c(t_f)$, such that the “population” in the initial and final instantaneous Jordan blocks are same but admitting transitions at the intermediate times. Based on the general solution Eq.(3), the complex phases $\eta_\alpha(t)$ are chosen as arbitrary functions to write down the time-evolution superoperator $\hat{\mathcal{E}}(t)$ as

$$\hat{\mathcal{E}}(t) = \sum_{\alpha=0}^{m-1} \exp(\eta_\alpha(t)) |\Phi_\alpha(t)\rangle\langle\langle\Phi_\alpha(0)|,$$

where $\langle\langle\Phi_\alpha(t)|$ is a left vector of the α -th Jordan block, which satisfies $\langle\langle\Phi_\beta(t)|\Phi_\alpha(t)\rangle\rangle = \delta_{\alpha\beta}$. The evolution superoperator obeys

$$\partial_t \hat{\mathcal{E}}(t) = \hat{\mathcal{L}}_c(t) \hat{\mathcal{E}}(t),$$

which we formally solve for the control Liouvillian

$$\hat{\mathcal{L}}_c(t) = \partial_t \hat{\mathcal{E}}(t) \hat{\mathcal{E}}^{-1}(t),$$

with

$$\hat{\mathcal{E}}^{-1}(t) = \sum_{\alpha=0}^{m-1} \exp(-\eta_\alpha(t)) |\Phi_\alpha(0)\rangle\langle\langle\Phi_\alpha(t)|.$$

Thus, we can express the control Liouvillian superoperator as

$$\begin{aligned} \hat{\mathcal{L}}_c(t) &= \\ &\sum_{\alpha=0}^{m-1} (\langle\partial_t \Phi_\alpha(t)|\langle\langle\Phi_\alpha(t)| + \partial_t \eta_\alpha(t) |\Phi_\alpha(t)\rangle\langle\langle\Phi_\alpha(t)|) \quad (5) \end{aligned}$$

Note that for a given dynamical invariant, there are many possible Liouvillians corresponding to different choices of complex phases $\eta_\alpha(t)$. In general, $\hat{\mathcal{I}}(0)$ does not commute with $\hat{\mathcal{L}}_c(0)$, which implies that the Jordan blocks of $\hat{\mathcal{I}}(0)$ do not coincide with the Jordan blocks of $\hat{\mathcal{L}}_c(0)$. $\hat{\mathcal{L}}_c(t_f)$ does not necessarily commute with $\hat{\mathcal{I}}(t_f)$ either. We impose $[\hat{\mathcal{I}}(0), \hat{\mathcal{L}}_c(0)] = [\hat{\mathcal{I}}(t_f), \hat{\mathcal{L}}_c(t_f)] = 0$, such that the Jordan blocks coincide and then the quantum state transfer from the initial block to the final one is guaranteed. Here, we must emphasize that $|\Phi_\alpha(t)\rangle$ can be arbitrary superposition of the right basis vectors $\{|D_\alpha^{(i)}(t)\rangle\}_{i=0}^{n_\alpha-1}$ for the α -th Jordan block. In other words, if the quantum state is prepared in a given Jordan block of $\hat{\mathcal{L}}_c(0)$ at the beginning and the final state is still in the same block of $\hat{\mathcal{L}}_c(t_f)$, the shortcuts to adiabaticity of open quantum systems is established, which is the control Liouvillian given by Eq.(5) designed to. This is the first result of this paper.

In Appendix. B, we present a detailed comparison between the STAs scheme and the transitionless quantum driving scheme of open quantum systems[15]. It is shown that, if the trajectory of the STAs scheme of open quantum systems is chosen as the adiabatic trajectory, the STAs scheme is coincident with the transitionless quantum driving method proposed in Ref.[15]. However, the adiabatic trajectory is not the only choice of the trajectories in our scheme. There are many trajectories can be used to inversely engineer the open quantum system. Proper trajectories always provide reasonable and applicable control protocols, which helps us to overcome the difficulties met in the control of microscopic or/and mesoscopic systems.

B. Mixed-state inverse engineering

In a practical application, the general control Liouvillian presented in Eq.(5) will meets difficulties in giving practical and affirmatory control protocols. In addition, most of eigenvectors of the control Liouvillian $\hat{\mathcal{L}}_c(t)$ are unphysical quantum states, except the eigenvectors with zero eigenvalues, which corresponds to steady states of open quantum systems. Therefore, for practical applications, we focus our attention on the steady states engineering of open quantum systems. Even if we restricts our discussion on speeding up the adiabatic steady state process, it is still difficult to obtain feasible control protocols [16], since the control Liouvillian Eq.(5) is in form of the superoperator. In the following, we propose an effective and practical method to obtain feasible control protocols, which is easy to be used in experiment.

We consider a quantum system with N -dimensional Hilbert space govern by a linear, time-local master equation

$$\begin{aligned}\partial_t \rho(t) &= \hat{\mathcal{L}}_0(t)[\rho(t)] \\ &= -\frac{i}{\hbar}[H_0(t), \rho] + \sum_{\alpha} \hat{\mathcal{D}}[L_{\alpha}](\rho),\end{aligned}$$

where $\hat{\mathcal{L}}_0(t)$ is the reference Liouvillian in the Lindblad form, $H_0(t)$ is the Hamiltonian, and

$$\hat{\mathcal{D}}[L_{\alpha}](\rho) = L_{\alpha}(N_{\alpha})\rho L_{\alpha}^{\dagger}(N_{\alpha}) - \frac{1}{2}\{L_{\alpha}^{\dagger}(N_{\alpha})L_{\alpha}(N_{\alpha}), \rho\} \quad (6)$$

is the Lindbladian. The Lindblad operators $L_{\alpha}(N_{\alpha})$ are related to some parameters $\{N_{\alpha}\}$, such as the decoherence rates and the temperatures of the environments. Here, we do not limit the master equation to be Markovian, but the corresponding evolution must be a completely positive trace-preserving map. Further, we assume that $\hat{\mathcal{L}}_0(t)$ admits an unique (instantaneous) steady state $\rho_0(t)$, which satisfies

$$\hat{\mathcal{L}}_0(t)[\rho_0(t)] = 0.$$

For practical applications, we focus our attention on speeding up the adiabatic steady state process[11], and seek the control Liouvillian from Eq.(2) directly. Concretely, the control task is to drive the open quantum system from the steady state of an initial Liouvillian $\hat{\mathcal{L}}_0(0)$ to the target one $\hat{\mathcal{L}}_0(t_f)$ [10, 11]. In order to achieve such purpose, we consider that the invariant has only one 1-dimensional Jordan block with non-zero eigenvalue Ω_I . If we set $|\Phi_0(0)\rangle\rangle = |\rho_0(0)\rangle\rangle$ and $|\Phi_0(t_f)\rangle\rangle = |\rho_0(t_f)\rangle\rangle$, the eigenvector $|\Phi_0(t)\rangle\rangle$ corresponds to the trajectory connecting the initial steady state and the target steady state. In general, we need to parameterize $\hat{\mathcal{I}}(t)$ in N^2 -dimensional Hilbert-Schmidt space with N^4 independent coefficients [16]. For the MIE scheme, since $|\Phi_0(t)\rangle\rangle$ should be a quantum state of the open quantum system, we can expand $|\Phi_0(t)\rangle\rangle$ by right vectors $\{|T_{\mu}\rangle\rangle\}_{\mu=1}^{N^2-1}$ which correspond to the $SU(N)$ Hermitian generators $\{T_{\mu}\}_{\mu=1}^{N^2-1}$, i.e.,

$$|\Phi_0(t)\rangle\rangle = \frac{1}{N} \left(|I\rangle\rangle + \sqrt{\frac{N(N-1)}{2}} \sum_{\mu=1}^{N^2-1} r_{\mu} |T_{\mu}\rangle\rangle \right), \quad (7)$$

where $\vec{r} = (r_1, r_2, \dots, r_{N^2-1})$ is the generalized Bloch vector with $\sum_{\mu} |r_{\mu}|^2 < 1$, and $|I\rangle\rangle$ is the right vector corresponding to a $N \times N$ identical operator. Thus, the dynamical invariants used in the MIE scheme can be defined as

$$\hat{\mathcal{I}}(t) = \Omega_I |\Phi_0(t)\rangle\rangle \langle\langle I|, \quad (8)$$

where Ω_I is an arbitrary nonzero constant and $\langle\langle I|$ is the left vector corresponding to a $N \times N$ identity matrix. With this notation, we can parameterize the dynamical invariant $\hat{\mathcal{I}}(t)$ with only N^2-1 parameters, which greatly simplifies the procedure in formulating control protocols.

To formulate feasible control protocols, we impose the control Liouvillians take the form as

$$\hat{\mathcal{L}}_c[\bullet] = -\frac{i}{\hbar}[H(t), \bullet] + \sum_{\alpha} \hat{\mathcal{D}}[L_{\alpha}](\bullet), \quad (9)$$

in which the Lindbladians and the Hamiltonian are chosen according to the following principles: (i) The Lindbladians in the control Liouvillian $\hat{\mathcal{L}}_c(t)$ have the same form as Eq.(6), which controls the system through control parameters $\{N_{\alpha}\}$. (ii) The control can also exert on the system via the Hamiltonian in $\hat{\mathcal{L}}_c(t)$. As it can be written in terms of $SU(N)$ Hermitian generators $\{T_k\}$, i.e.,

$$H(t) = \sum_{k=1}^{N^2-1} c_k(t) T_k,$$

we might choose $\{c_k(t)\}$ as the control parameters to manipulate the system. In this way, the control Liouvillians can always present feasible control protocols. Substituting $\hat{\mathcal{L}}_c(t)$ and $\hat{\mathcal{I}}(t)$ into Eq.(2), we can express the

control parameters $\{c_k, N_\alpha\}$ as a function of the generalized Bloch vector and its derivative $\{r_\mu, \partial_t r_\mu\}$. On the other hand, the control Liouvillian is always the same as the reference Liouvillian at the initial and final moment, which leads to boundary conditions for $\{r_\mu, \partial_t r_\mu\}$. By utilizing the control parameters $\{c_k, N_\alpha\}$ and setting proper boundary conditions for $\{r_\mu, \partial_t r_\mu\}$, the open quantum system can be transferred from the initial steady state into the target steady state along an exact trajectory given by $|\Phi_0(t)\rangle\rangle$. This is the second result of this paper.

If some control parameters, say $\{\tilde{c}_k, \tilde{N}_\alpha\}$, are difficult to implement in a real setting, we can single out the equations for those parameters, and force them to be some values which are available in the experimental setting. Notice that the equations for $\{\tilde{c}_k, \tilde{N}_\alpha\}$ are about the components of the trajectory $\{r_\mu, \partial_t r_\mu\}$. Thus picking up proper $\{\tilde{r}_\mu\}$ to be free components in trajectory, we obtain a set of differential equations about $\{\tilde{r}_\mu\}$. Solving those differential equations is equivalent to choose a trajectory with particular components $\{\tilde{r}_\mu\}$. Therefore the MIE scheme can avoid those difficulties encountered in the control process, such as the negative decoherence rate[21] and the impractical energy-levels couplings[6]. As a result, the MIE offers a practical method to engineer an open quantum system with an exact trajectory which can be realized in laboratory with current technology.

III. EXAMPLE: THE STIMULATED RAMAN ADIABATIC PASSAGE (STIRAP)

Consider a single nitrogen-vacancy (NV) center in diamond, which hosts a solid-state Λ system. The NV center has a spin-triplet, orbital-singlet ground state (3A_2) that is coupled optically to a spin-triplet, orbital-doublet excited state (3E), as shown in Fig. 1 (a). The experiments have had identified the three singlet states (1E , 1A_1) [22], where 1E is double degenerate.

For the negative charged NV center with electron spin $S = 1$, the ground state is a spin-triplet state with a zero-field splitting $D_0 = 2.87$ GHz between spin sublevels $|m_s = 0\rangle$ and $|m_s = \pm 1\rangle$ due to electronic spin-spin interaction. Applying a static magnetic field B_{NV} along the NV axis splits the $|m_s = -1\rangle$ and $|m_s = +1\rangle$ ground states by $2\gamma_{NV}B_{NV}$ with $\gamma_{NV} = 2.8$ MHz G $^{-1}$. Passing single tunable laser (637.2 nm) through a phase electro-optic modulator produce frequency harmonics to resonantly excite both $|m_s = -1\rangle$ and $|m_s = +1\rangle$ to the spin-orbit excited state $|A_2\rangle$, which is used as the intermediate state for STIRAP. After the modulation of an amplitude electro-optic modulator with a 10 GHz arbitrary wave form generator produces the control fields $\Omega_s(t)$ and $\Omega_p(t)$ used in STIRAP. The Hamiltonian within the rotating wave approximation can be expressed in the basis

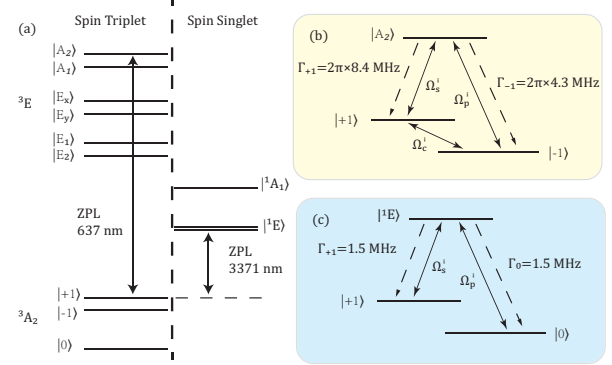


FIG. 1. The level structure of the NV center. (a) A schematic illustration of the level structure of the NV centers. The optical zero photon line (ZPL) at 637 nm is related to the transition from 3E to 3A_2 and the ZPL at 3371 nm corresponds to the transition from 1E to 3A_2 . (b) State transfer in a NV centre Λ system by the protocol with initial-to-final state coupling. (c) State transfer in a NV centre Λ system by the protocol without the initial-to-final state coupling.

$\{|m_s = -1\rangle, |A_2\rangle, |m_s = +1\rangle\}$ by a matrix[23],

$$H_0(t) = \frac{\hbar}{2} \begin{pmatrix} 0 & \Omega_p(t) & 0 \\ \Omega_p(t) & 0 & \Omega_s(t) \\ 0 & \Omega_s(t) & 0 \end{pmatrix}. \quad (10)$$

For simplify our discussion, the “one-photon resonance” case is considered. The shortcuts of the open STIRAP for a general case can be obtained with the same procedure. Here we assume that the adiabatic pulses satisfy

$$\Omega_s(t) = \Omega(t) \cos \theta(t), \quad \Omega_p(t) = \Omega(t) \sin \theta(t), \quad (11)$$

with $\tan \theta(t) = \Omega_p(t)/\Omega_s(t)$ and $\Omega(t) = \sqrt{\Omega_s^2(t) + \Omega_p^2(t)}$.

Consider that the Λ system couples to a bosonic heat reservoir at finite temperature T . The effect of the heat reservoir is to induce decay from $|A_2\rangle$ to $|m_s = \pm 1\rangle$. The decay rate are $\Gamma_{-1} = 2\pi \times 4.3$ MHz (from $|A_2\rangle$ to $|m_s = -1\rangle$) and $\Gamma_{+1} = 2\pi \times 8.5$ MHz (from $|A_2\rangle$ to $|m_s = +1\rangle$), as shown in FIG. 1 (b). Moreover, the orbital dephasing of the level $|A_2\rangle$ can not be ignored [24], where the dephasing rate is $\Gamma_d = 2\pi \times 8.8$ MHz. All of decoherence rates mentioned here are selected from the measurement in recent experiment[9]. The dynamics of the Λ system is governed by

$$\partial_t \rho(t) = \hat{\mathcal{L}}_0 \rho(t) + \Gamma_d \hat{D}[L_d] \rho(t), \quad (12)$$

where

$$\begin{aligned} \hat{\mathcal{L}}_0 \rho(t) = & -\frac{i}{\hbar} [H_0(t), \rho] \\ & + \sum_{\alpha=0,+1} \Gamma_\alpha ((N_\alpha + 1) \hat{D}[L_\alpha](\rho) + N_\alpha \hat{D}[L_\alpha^\dagger](\rho)). \end{aligned}$$

and $\hat{D}[L_\alpha](\rho) = L_\alpha(t) \rho L_\alpha^\dagger(t) - \frac{1}{2} \{L_\alpha^\dagger(t) L_\alpha(t), \rho\}$. For the decay form $|A_2\rangle$, the lindblad operators can be expressed

as $L_{\pm 1} = |m_s = \pm 1\rangle\langle A_2|$; and $L_d = |A_2\rangle\langle A_2|$ for the orbital dephasing. $N_\alpha = [\exp(\hbar\omega_{2\rightarrow\alpha}/kT) - 1]^{-1}$ denote the mean excitation numbers. In the following discussion, we choose $\hat{\mathcal{L}}_0$ as the reference Liouvillian, and the dephasing is the key obstacle for the performance of the protocol.

A. The Adiabatic Trajectory

In this subsection, we present the control protocol where the quantum state transfers along the adiabatic trajectory given by the instantaneous steady state of $\hat{\mathcal{L}}_0(t)$. We parameterize the instantaneous steady state of $\hat{\mathcal{L}}_0(t)$ via the generalized Bloch vector $\{r_k\}_{k=1}^8$. The density matrix of the three-level system can be written as,

$$\rho(t) = \frac{1}{3} \left(\mathbf{I} + \sqrt{3} \sum_{k=1}^8 r_k(t) T_k \right), \quad (13)$$

where \mathbf{I} is a 3×3 identity matrix, and T_k denotes the regular Gellmann matrix. These $\{T_k\}$ span all traceless Hermitian matrices of the Lie algebra $\text{su}(3)$. If $\Gamma_{+1} = \Gamma_{-1} \equiv \Gamma$ and $N_{+1} = N_{-1} \equiv N$, the components of the Bloch vector corresponding to the instantaneous steady state of $\hat{\mathcal{L}}_0(t)$ are

$$\begin{aligned} r_2 &= \sqrt{3} N \Gamma \Omega_p / z, \\ r_3 &= \sqrt{3} ((3N^2 + 2N) \Gamma^2 + \Omega_s^2) / (2z), \\ r_4 &= -\sqrt{3} \Omega_p \Omega_s / z, \\ r_7 &= -\sqrt{3} N \Gamma \Omega_s / z, \\ r_8 &= -((3N^2 + 2N) \Gamma^2 + 2\Omega_p^2 - \Omega_s^2) / (2z), \end{aligned} \quad (14)$$

with $z = (3N + 1) \Omega^2 + N \Gamma^2 (3N + 2)^2$, and the other components are zeros. The details for obtaining the instantaneous steady state can be found in Appendix C. Correspondingly, the dynamical invariants can be expressed by the Bloch vector according to the MIE scheme (see Eq.(8)),

$$\hat{\mathcal{I}}(t) = \Omega_I |\rho_0\rangle\langle\langle \mathbf{I}|, \quad (15)$$

where Ω_I is an arbitrary nonzero constant and $\langle\langle \mathbf{I}|$ is the left vector corresponding to a 3×3 identity matrix.

Assume that the total Liouvillian reads

$$\hat{\mathcal{L}} = \hat{\mathcal{L}}_c + \Gamma_d \hat{\mathcal{D}}[L_d]. \quad (16)$$

The control Liouvillian has the same form as Eq.(12),

$$\begin{aligned} \hat{\mathcal{L}}_c \rho(t) &= -i[H_c(t), \rho] \\ &+ \sum_{\alpha=\pm 1} \Gamma_\alpha ((N_\alpha^i + 1) \hat{\mathcal{D}}[L_\alpha](\rho) + N_\alpha^i \hat{\mathcal{D}}[L_\alpha^\dagger](\rho)), \end{aligned} \quad (17)$$

where the Hamiltonian is

$$H_c(t) = \frac{\hbar}{2} \begin{pmatrix} 0 & \Omega_p^i(t) & i\Omega_c^i(t) \\ \Omega_p^i(t) & 0 & \Omega_s^i(t) \\ -i\Omega_c^i(t) & \Omega_s^i(t) & 0 \end{pmatrix}. \quad (18)$$

Here we also assume that the mean excitation numbers $N_{\pm 1}^i$ are tunable independently, which can be achieved by properly engineering the temperature of the environment [25] or shifting the energy difference between $|A_2\rangle$ and $|m_s = \pm 1\rangle$. Substituting Eqs. (15) and (17) into Eq.(2), we can determine all the control parameters in the control Liouvillian $\hat{\mathcal{L}}_c$. The analytical expression of these control parameters are presented in Appendix D. Alternatively, these control parameters can be obtained numerically, especially for more complex situation such as $\Gamma_{-1} \neq \Gamma_{+1}$. Taking Eq.(11) and Eqs.(14) into the analytical expressions, we obtain the control parameters for the adiabatic trajectory with a time-independent Ω ,

$$\begin{aligned} \Omega_s^i &= \Omega \sin(\theta(t)), \quad \Omega_p^i = \Omega \cos(\theta(t)), \quad \Omega_c^i = \partial_t \theta(t), \\ N_{-1}^i &= N, \quad N_{+1}^i = N. \end{aligned}$$

These control parameters are exactly the parameters obtained in the transitionless quantum driving scheme of closed systems for the STIRAP[6].

Despite the MIE scheme and the transitionless driving scheme of closed systems provide similar control protocols for an adiabatic trajectory, their essences are quite different. The two schemes give similar control protocols only if $\Omega = \sqrt{\Omega_s^2(t) + \Omega_p^2(t)}$ is time-independent. This can be illustrated by the spectrum decomposition of the instantaneous steady state of $\hat{\mathcal{L}}_0$. The eigenvalues of ρ_0 are

$$\begin{aligned} p_1 &= \frac{1}{z} \left((2N+1)(3N+2)N\Gamma^2 + 2N\Omega^2 \right. \\ &\quad \left. - N\Gamma\sqrt{(3N+2)^2\Gamma^2 + 4\Omega^2} \right), \\ p_2 &= \frac{1}{z} \left((2N+1)(3N+2)N\Gamma^2 + 2N\Omega^2 \right. \\ &\quad \left. + N\Gamma\sqrt{(3N+2)^2\Gamma^2 + 4\Omega^2} \right), \\ p_3 &= \frac{(N+1)}{z} ((3N+2)N\Gamma^2 + \Omega^2). \end{aligned}$$

with $z = (3N+1)\Omega^2 + N\Gamma^2(3N+2)^2$, which denote the populations on corresponding eigenstates. If Ω is constant, the population on every eigenstate is invariant, so that a unitary evolution is enough to transfer the quantum state into the target steady state. But if Ω is time-dependent, the incoherent controls are required for the STIRAP process along the adiabatic trajectory because of time-varying purity of the quantum state.

Figures 2 (a) and (b) show the control fields and the corresponding population for the open Λ system at room temperature (300K). The corresponding mean excitation number is $N = 1.9 \times 10^{-33}$. The boundary conditions of $\theta(t)$ are set to be $\theta(0) = 0$ and $\theta(\tau) = \pi/2$. We choose the simplest STIRAP pulses, i.e., $\theta(t) = \pi t/(2\tau)$, where τ is the pulse length. The numerical results of the control fields show that, for nonadiabatic state transfer along the adiabatic trajectory, the control protocol is completely

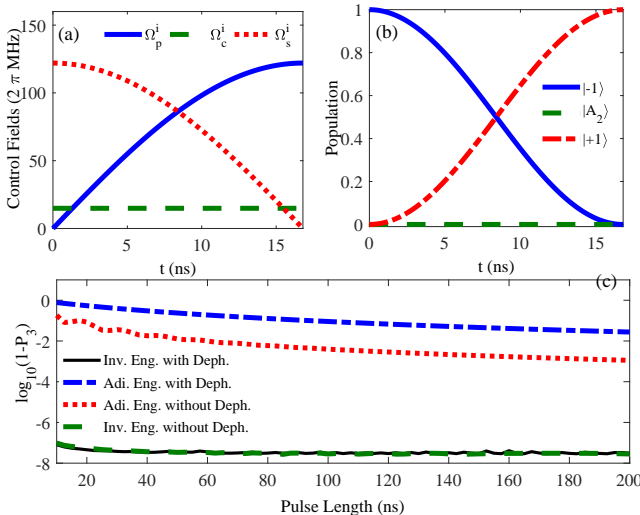


FIG. 2. (a) The control field and (b) the population on $|m_s = -1\rangle$ (blue solid line), $|A_2\rangle$ (green dash line), and $|+1\rangle$ (red dot-dash line) as a function of time for pulses length $\tau = 16.8$ ns, (c) the final population on states except $|m_s = +1\rangle$ as a function of the pulse length τ for $\Omega = 2\pi \times 122$ MHz, $\Gamma_{-1} = 2\pi \times 4.3$ MHz, $\Gamma_{+1} = 2\pi \times 8.4$ MHz, $\Gamma_d = 2\pi \times 8.8$ MHz, and $N = 1.9 \times 10^{-33}$.

the same as the protocol given by the transitionless quantum driving method [6]. This illustrates that the transitionless driving method [26, 27] will present a better transfer efficiency than any other scheme else[9, 28], if Ω is set to be constant. As shown in FIG.2 (b), the quantum state is transferred into the target state with a perfect final population. In FIG. 2 (c), we plot the final population not on $|m_s = +1\rangle$ (denoted by $\log_{10}(1 - P_3)$) with $P_3 = \langle m_s = +1 | \rho(\tau) | m_s = +1 \rangle$ as a function of the pulse length τ for both the adiabatic scheme (the red dots and blue dot-dash lines) and the MIE scheme (green dash and black solid lines). Comparing to the adiabatic scheme, our scheme can transfer the population into $|m_s = +1\rangle$ with transfer efficiency very close to 1(at least 10^{-6} , see the figure). Since $|A_2\rangle$ is unoccupied, our protocol is immune to the orbital dephasing encountered in the earlier proposals.

In practical applications, the initial-to-final state coupling Ω_c^i can be implemented in some but not in all systems, e.g., because of selection rules due to symmetry of the states or the necessary phase of the term. In nitrogen-vacancy electronic spins, this additional coupling was implemented mechanically via a strain field in the recent experiment [29, 30]. The strain field to drive NV spins is based on the sensitive response of the NV spin states to strain in the diamond host lattice. For uniaxial strain applied transverse to the NV axis, the transverse strain field couples the electronic spin states $|m_s = -1\rangle$ and $|m_s = +1\rangle$. To realize such strain field for efficient coherent driving, a mechanical resonator is required in the form of a singly clamped, single-crystalline diamond can-

tilever, in which the NV center is directly embedded [30]. The cantilever is actuated at its mechanical resonance frequency $\omega_m = 2\pi \times 6.84$ MHz. Thus, for resonance driving, the external magnetic field satisfies $B_{NV} = 2.42$ G. And the corresponding Rabi frequency is characterized by $\Omega_c = \gamma_T x_c / x_{zpf}$, where γ_T is the transverse single-phonon strain-coupling strength, x_c and x_{zpf} are the cantilever zero-point fluctuation and peak amplitude, respectively (with $\gamma_T \sim 2\pi \times 0.08$ MHz and $x_{zpf} \sim 7.7 \times 10^{-15}$ m). Therefore, we can tune the cantilever's amplitude x_c to adjust the Rabi frequency of the strain field.

B. The Trajectory without Initial-to-Final State Couplings

In experiment, a initial-to-final state coupling induced by the strain field $\Omega_c^i(t)$ can be realized in artificial structure but not in real atoms via dipole-dipole coupling due to the selection rule. The pure-state inverse engineering scheme solves this by providing alternative shortcuts that do not couple directly levels $|m_s = -1\rangle$ and $|m_s = +1\rangle$ [19]. In the following, we show that the MIE scheme has the same quality via selecting a proper trajectory of the quantum state. And this particular trajectory can be obtained only by solving differential equations about the components of the Bloch vector, but not to design a complex transformation of the entire trajectory as done in the STAs schemes of closed quantum systems. More importantly, our protocol is robust to the decay and dephasing noise at the same time.

We consider the case where the Stocks pulse and the pumping pulse resonantly excite both $|m_s = 0\rangle$ and $|m_s = +1\rangle$ to the excited-state spin singlet ${}^1E\rangle$, as shown in FIG. 1 (c). The singlet-ground ($|m_s = 0\rangle \rightarrow {}^1E\rangle$) splitting is about 89 THz. The decay from the singlet state to the ground states is spin-nonpreserving nonradiative decay. The corresponding decay rates depend on the static magnetic field \mathbf{B}_{NV} with an angle η with respect to the NV defect axis. It has been shown that the decay rates are approximatively equal for $\eta = \pi/10$, and have been measured in the lab with the results $\Gamma_0 \approx \Gamma_{+1} = 2\pi \times 1.5$ MHz [32]. Moreover, due to spin-nonpreserving decay, the effective rate of the population excitation from $|m_s = 0\rangle$ to ${}^1E\rangle$ is much lower than the decay rate from ${}^1E\rangle$ to $|m_s = 0\rangle$, while the effective rate from the $|m_s = +1\rangle$ to ${}^1E\rangle$ is almost equal to its corresponding decay rate. This results that the $|m_s = +1\rangle - {}^1E\rangle$ and $|m_s = 0\rangle - {}^1E\rangle$ subsystems can be seen as coupling to two different thermal reservoirs [31]. It has also been shown in Ref. [31] that tuning the strength of \mathbf{B}_{NV} can effectively engineer temperatures of the thermal reservoirs.

In order to cancel the initial-to-final state coupling, the control field $\Omega_c^i(t)$ must be zero at any point in time. A direct manner is to modify the trajectory of the quantum state. Here, we consider the case where the decay rates are equal. As illustrated in the analytical expressions

of the control parameters (see Appendix. D), $\Omega_c^i(t)$ can be written as a function of the Bloch vector and its time derivative $\{r_i, \partial_t r_i\}_{i=1}^8$. What we may do is to force $r_4(t)$ to vary in a proper way such that $\Omega_c^i(t) = 0$. To be specific, we consider the requirement $\Omega_c^i(t) = 0$ as a restriction to solve the differential equation of $r_4(t)$, keeping other components of the Bloch vector unchanged. This would finally leads to a proper trajectory that cancels the initial-to-final state coupling.

By choosing a trajectory according to the instantaneous steady state of $\hat{\mathcal{L}}_0$ (see Appendix. E), we plot the control parameters and the populations as a function of time in FIG. 3. We notice that the additional coupling $\Omega_c^i(t)$ is eliminated in the engineering process (the green solid line in FIG. 3 (a)), and the population is transferred from $|m_s = 0\rangle$ into the target state $|m_s = +1\rangle$ with high transfer efficiency as shown in FIG. 3 (c). In addition, the excitation numbers of the reservoirs need to be engineered accordingly (see FIG. 3 (b)).

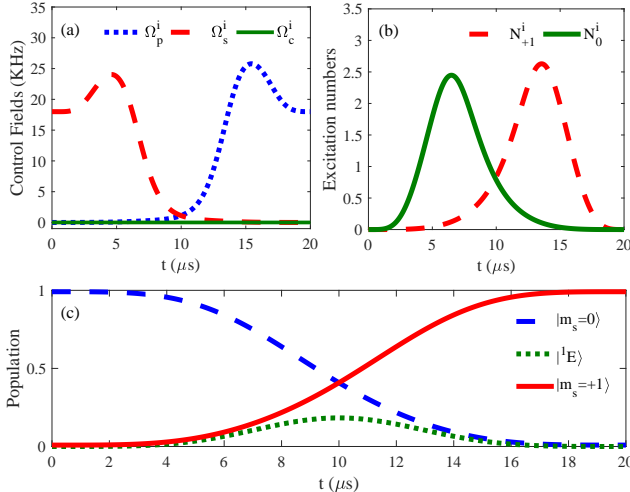


FIG. 3. (a) The control fields, (b) the mean excitation numbers, and (c) the population on states $|m_s = 0\rangle$ (blue lines), $|^1E\rangle$ (green lines), and $|m_s = +1\rangle$ (red lines) as a function of time for $\Omega = 18.1$ KHz, $\Gamma = 2\pi \times 1.5$ MHz, $\Gamma_d = 2\pi \times 8.8$ MHz, and $N = 6.55 \times 10^{-7}$. The pulses length is $\tau = 20 \mu$ s.

Although FIG. 3 presents positive main excitation numbers, these main excitation numbers may still negative at some points of the time. In experiment, we may restrict the main excitation numbers to be within the regime $N_0^i, N_{+1}^i \geq 6.55 \times 10^{-7}$ which corresponds to $T_{\text{cutoff}} \approx 300$ K. In FIG. 4(a), we plot the final population which is not on $|m_s = +1\rangle$ as a function of the pulse length τ for the control field $\Omega = 154$ KHz. Both dynamical processes with (the red dash line) and without (the blue solid line) the dephasing noise are considered in FIG.4. As we see, the MIE scheme fails to transfer the population into $|m_s = +1\rangle$ for short pulse length due to the cut-off on the main excited number N_{+1}^i . But it performs good by prolonging pulse length, and the final

population on $|m_s = +1\rangle$ approach asymptotically to a predicted value give by the instantaneous steady state of $\hat{\mathcal{L}}_0(\tau)$. On the other hand, since the coherence between $|^1E\rangle$ and $|m_s = 0\rangle$ ($|m_s = +1\rangle$) in our designed trajectory is negligible, the orbital dephasing noise of $|^1E\rangle$ will not affect the state transfer process evidently. The numerical result confirms our analysis as illustrated by the blue solid line and the red dash line in FIG. 4 (a). We also present the results given by the superadiabatic scheme[30] with (the green dots line) and without (the black dash-dot line) the dephasing noise. As a pure-state STAs scheme, the superadiabatic scheme needs to keep states as pure states. When $|^1E\rangle$ is populated, the strong coherence between the excited and ground states are required, so that pure-state STAs schemes are sensitive to the dephasing noise. Therefore, the MIE scheme is more robust to the orbital dephasing noise than the STAs schemes of closed quantum systems.

We also plot the population on all states except $|m_s = +1\rangle$ (blue solid line) as a function of the control field Ω with a pulse length $\tau = 5 \mu$ s in FIG. 4 (c). As expected, the final population on $|m_s = +1\rangle$ increases with the control field. The population not on $|m_s = +1\rangle$ given by the steady state $\rho_0(\tau)$ is also plotted, see the green dash line. We find that the final population for the inverse engineering can not reach the predicted value due to the main excitation number cutoff, see FIG. 4 (d). As illustrated by the red dot line in FIG. 4 (c), the worst deviation of the final population is no more than 10^{-4} . Therefore, although the final population deviates from the predicted value, we can still obtain a satisfactory transfer efficiency in the regime of strong control field.

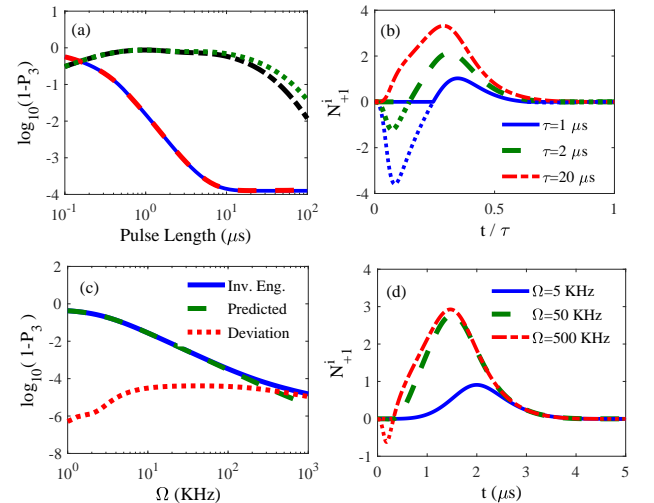


FIG. 4. The final population not on $|m_s = +1\rangle$ (red lines) as a function of (a) the pulse length τ for $\Omega = 154$ KHz and (c) the control fields Ω for $\tau = 5 \mu$ s. The main excitation number N_{+1}^i as a function of time with (b) different pulse length for $\Omega = 154$ KHz and (d) different control fields for $\tau = 5 \mu$ s. The other parameters in the master equation are chosen as $\Gamma = 2\pi \times 1.5$ MHz, $\Gamma_d = 2\pi \times 8.8$ MHz, and $N = 6.55 \times 10^{-7}$.

IV. COMPARISON WITH THE PURE-STATE INVERSE ENGINEERING SCHEME

A. Pure-state Engineering

In this section, we compare the MIE scheme to the pure-state inverse engineering (PIE) scheme. Firstly, we show that the STAs scheme of open quantum systems includes the PIE scheme. To inversely engineering a pure-state, the dynamical invariants $I(t)$ of closed systems are needed[18], which satisfies

$$i \partial_t I(t) = [H(t), I(t)],$$

with the Hamiltonian $H(t)$. The general solution of closed systems can be written as

$$|\Psi(t)\rangle = \sum_n c_n \exp(i\alpha_n(t)) |\psi_n(t)\rangle, \quad (19)$$

where c_n are time-independent amplitudes, $|\psi_n(t)\rangle$ are orthonormal eigenvectors of the invariant $I(t)$, and $\alpha_n(t)$ are the Lewis-Riesenfeld phases. According to the general solution Eq.(19), we can write down the time-dependent unitary evolution operator U as

$$U(t) = \sum_n \exp(i\alpha_n(t)) |\psi_n(t)\rangle \langle \psi_n(0)|,$$

which obeys

$$i \partial_t U(t) = H(t) U(t).$$

Thus, we obtain the formal expression of the Hamiltonian as

$$H(t) = \sum_n (i |\partial_t \psi_n(t)\rangle \langle \psi_n(t)| - \partial_t \alpha_n(t) |\psi_n(t)\rangle \langle \psi_n(t)|). \quad (20)$$

If we impose $[H(0), I(0)] = [H(\tau), I(\tau)] = 0$, the eigenstates coincide and then a state transfer from a initial eigenstate of the Hamiltonian to the final one is guaranteed.

For applying the STAs scheme of open quantum systems to a pure-state engineering task, we can formulate the dynamical invariant superoperator $\hat{\mathcal{L}}$ by the eigenstates of closed systems' dynamical invariant. The time-dependent eigenstates of $\hat{\mathcal{L}}$ are chosen as

$$|\Psi_{mn}\rangle = |\psi_m\rangle \otimes |\psi_n^*\rangle, \quad (21)$$

which corresponds to the time-independent eigenvalues λ_{mn} . Substituting $\{|\Psi_{mn}\rangle\}$ into Eq.(5), the control Liouvillian superoperator can be obtained with arbitrary phases $\eta_{mn}(t)$. Thus, $\hat{\mathcal{L}}_c(t)$ transfers the quantum state from $|\psi_n(0)\rangle$ to $|\psi_n(\tau)\rangle$ along with $|\Psi_{nn}(t)\rangle$. According to Eq.(5), the control Liouvillian can be written as

$$\hat{\mathcal{L}}_c(t) = \sum_{mn} (|\partial_t \Psi_{mn}\rangle \langle \Psi_{mn}| + \partial_t \eta_{mn} |\Psi_{mn}\rangle \langle \Psi_{mn}|).$$

By considering Eq.(21), it yields

$$\begin{aligned} \hat{\mathcal{L}}_c(t) = & \sum_{mn} (|\partial_t \psi_m\rangle \langle \psi_m| \otimes (|\psi_n\rangle \langle \psi_n|)^* \\ & + |\psi_m\rangle \langle \psi_m| \otimes (\partial_t |\psi_n\rangle \langle \psi_n|)^* \\ & + \partial_t \eta_{mn} |\Psi_{mn}\rangle \langle \Psi_{mn}|). \end{aligned}$$

Since $\{|\psi_m\rangle\}$ is a complete set of the Hilbert space, we have

$$\begin{aligned} \hat{\mathcal{L}}_c(t) = & -i \left(\sum_{mn} \partial_t \eta_{mn} |\Psi_{mn}\rangle \langle \Psi_{mn}| \right. \\ & \left. + \left(\sum_m i |\partial_t \psi_m\rangle \langle \psi_m| \otimes \mathbf{I} - \mathbf{I} \otimes \left(\sum_n i \partial_t |\psi_n\rangle \langle \psi_n| \right)^* \right) \right). \end{aligned}$$

where \mathbf{I} is an identity matrix. If we choose the phase satisfies $\eta_{mn} = i(\alpha_m - \alpha_n)$, it can be obtained that

$$\begin{aligned} \hat{\mathcal{L}}_c(t) = & -i \left(\left(i \sum_m |\partial_t \psi_m\rangle \langle \psi_m| - \partial_t \alpha_m |\partial_t \psi_m\rangle \langle \psi_m| \right) \otimes \mathbf{I} \right. \\ & \left. - \mathbf{I} \otimes \left(i \sum_n \partial_t |\psi_n\rangle \langle \psi_n| - \partial_t \alpha_n |\partial_t \psi_n\rangle \langle \psi_n| \right)^* \right). \end{aligned}$$

Considering the map from the superoperator to operators: $A \otimes B^* |\rho\rangle \mapsto A \rho B^\dagger$ for arbitrary operators A and B , we immediately have

$$\hat{\mathcal{L}}_c(t) |\rho(t)\rangle = -i [H(t), \rho(t)], \quad (22)$$

where $H(t)$ is just the Hamiltonian involved in the PIE scheme as shown in Eq.(20). Therefore, the STAs scheme of open quantum systems includes the PIE scheme.

In the following, we take the STIRAP as an example to show that the STAs scheme gives same control protocol as the PIE scheme. Following the step of Ref.[19], the eigenstates of dynamical invariant are given by

$$\begin{aligned} |\psi_0\rangle &= \begin{pmatrix} \cos \gamma \cos \beta \\ -i \sin \gamma \\ -\cos \gamma \sin \beta \end{pmatrix}, \\ |\psi_\pm\rangle &= \frac{\sqrt{2}}{2} \begin{pmatrix} \sin \gamma \cos \beta \pm i \sin \beta \\ i \cos \gamma \\ -\sin \gamma \sin \beta \pm i \cos \beta \end{pmatrix}. \end{aligned}$$

Thus, we can formulate the eigenstate of the dynamical invariant superoperator according to Eq.(21). Substituting Eq.(21) into Eq.(5), we obtain the control Liouvillian $\hat{\mathcal{L}}_c$ as a function of β , γ , and phases η_{mn} . Comparing η_{mn} with the Lewis-Riesenfeld phases α_n , we immediately find that $\eta_{mn} = i(\alpha_m - \alpha_n)$. Thus, we have $\eta_{nn} = 0$, $\eta_{+-} = -\eta_{-+} \equiv \eta_1$, $\eta_{+0} = -\eta_{0+} \equiv \eta_2$, and $\eta_{0-} = -\eta_{-0} \equiv \eta_3$. The control Liouvillian can be expanded by SU(3) generators (T_i - the regular Gellmann matrixes Eq.(C3)), i.e.,

$$\hat{\mathcal{L}}_c(t) = \sum_{i,j=1}^9 c_{ij} T_i \otimes T_j^*.$$

where T_9 is a 3×3 identity matrix. c_{ij} is time-dependent expanding coefficients, which can be determined by

$$c_{ij} = \text{Tr}(\hat{\mathcal{L}}(t)T_i \otimes T_j^*).$$

$$c = \frac{i}{2} \times \begin{pmatrix} 0 & 0 & 0 & 0 & 0 & -2\partial_t\gamma \cos \beta - \eta_1 \cos \gamma \sin \beta \\ 0 & 0 & 0 & 0 & 0 & 0 \\ 0 & 0 & 0 & 0 & 0 & 0 \\ 0 & 0 & 0 & 0 & 0 & 0 \\ 0 & 0 & 0 & 0 & 0 & 2\partial_t\beta - \eta_1 \sin \gamma \\ 0 & 0 & 0 & 0 & 0 & 2\partial_t\gamma \sin \beta - \eta_1 \cos \beta \cos \gamma \\ 0 & 0 & 0 & 0 & 0 & 0 \\ 0 & 0 & 0 & 0 & 0 & 0 \\ 2\partial_t\gamma \cos \beta + \eta_1 \cos \gamma \sin \beta & 0 & 0 & 0 & -2\partial_t\beta + \eta_1 \sin \gamma & -2\partial_t\gamma \sin \beta + \eta_1 \cos \beta \cos \gamma \end{pmatrix}.$$

In other words, the control Liouvillian reads

$$\begin{aligned} \hat{\mathcal{L}}_c(t) = & -i((2\partial_t\gamma \cos \beta + \eta_1 \cos \gamma \sin \beta)(T_1 \otimes T_9^* - T_9 \otimes T_1^*) \\ & + (2\partial_t\beta - \eta_1 \sin \gamma)(T_5 \otimes T_9^* - T_9 \otimes T_5^*) \\ & + (\eta_1 \cos \beta \cos \gamma - 2\partial_t\gamma \sin \beta)(T_6 \otimes T_9^* - T_9 \otimes T_6^*)). \end{aligned}$$

Thus, the control Liouvillian can be transformed as

$$\hat{\mathcal{L}}_c(t)|\rho(t)\rangle \mapsto -i[H(t), \rho(t)] \quad (23)$$

with $H(t) = \Omega_p/2 T_1 + \Omega_c/2 T_5 + \Omega_s/2 T_6$, in which the control fields are

$$\begin{aligned} \Omega_p &= \eta_1 \cos \gamma \sin \beta + 2\partial_t\gamma \cos \beta, \\ \Omega_c &= 2\partial_t\beta - \eta_1 \sin \gamma, \\ \Omega_s &= \eta_1 \cos \beta \cos \gamma - 2\partial_t\gamma \sin \beta. \end{aligned} \quad (24)$$

In order to cancel initial-to-final state couplings, the phase η_1 has to be selected as $\eta_1 = 2\partial_t\beta/\sin \gamma$. Taking η_1 into above equations, we immediately obtain the same control protocol given in Ref.[19], i.e.,

$$\begin{aligned} \Omega_p &= 2\partial_t\beta \cot \gamma \sin \beta + 2\partial_t\gamma \cos \beta, \\ \Omega_s &= 2\partial_t\beta \cot \gamma \cos \beta - 2\partial_t\gamma \sin \beta, \\ \Omega_c &= 0. \end{aligned} \quad (25)$$

Therefore, the STAs scheme of open quantum systems is equivalent to the PIE scheme if the control task is to transfer pure states with a pure-state trajectory.

B. Pure-state Engineering with Mixed-state Trajectories

The MIE scheme provides more feasible control protocols than the PIE scheme, because the trajectory does not have to be a pure-state trajectory. As illustrated by the STRIAP of open quantum systems, the robustness to the dephasing noise attributes to the mixed-state trajectory with weak coherence between the energy levels.

Moreover, if the phase η_k ($k = 1, 2, 3$) have following relation: $\eta_2 = \eta_1/2$ and $\eta_3 = -\eta_1/2$, it yields the coefficient matrix

In this subsection, we show that the MIE scheme overcomes the difficulties meeting in the PIE scheme. As shown in Eq.(25), $|^1E\rangle$ needs to be populated for avoiding infinitely large $\Omega_{p,s}$. The strengths of control fields satisfy $\Omega_{p,s} \propto 1/\sqrt{P_2}$ where $P_2 = \sin^2 \gamma$ is the population on $|^1E\rangle$. For the control protocol given by the MIE scheme, reasonable and feasible $\Omega_{p,s}$ are needed instead of infinitely large control fields, which is illustrated in FIG. 5 (a).

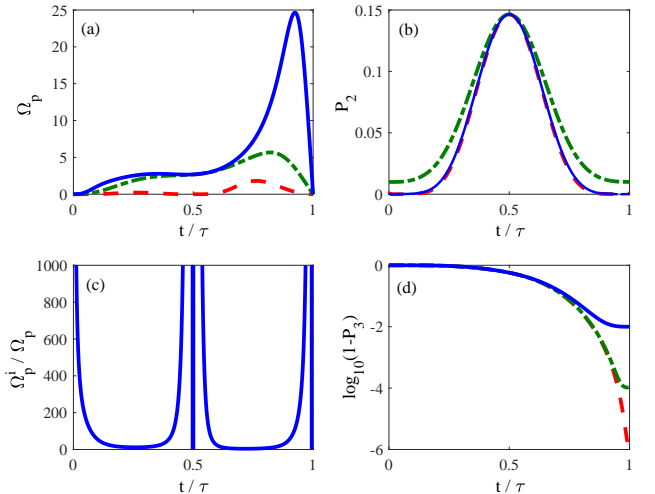


FIG. 5. (a) The control field Ω_p , (b) the population on $|^1E\rangle$, (c) the ratio of the control field strengths between the mixed-state and the pure-state inverse engineering schemes, and (d) the population out of $|+1\rangle$ vs the dimensionless time t/τ for the mixed-state trajectory (red dash lines) and the pure state trajectory with $\gamma_0 = 0.1$ (green dot-dash lines) and $\gamma_0 = 0.01$ (blue solid lines). The decay rate is chosen as $\Gamma = 10/\tau$.

For the control protocol given by the PIE scheme, the parameters in Eq.(25) is chosen as: $\gamma = (\gamma_m -$

$\gamma_0) \sin^3(\pi t/\tau) + \gamma_0$ with constants γ_m and γ_0 ; $\beta = \pi/2 \sin(\pi t/(2\tau))$. For the mixed-state protocol, we set a analogous trajectory with $r_3 = -\sqrt{3}(\sin^2 \gamma - \cos^2 \beta \cos^2 \gamma)/2$, $r_8 = (3 \sin^2 \gamma + 3 \cos^2 \beta \cos^2 \gamma - 2)/2$. Since the mixed-state protocol does not need the population on $|^1E\rangle$, we set $\gamma_0 = 0$ in the mixed-state trajectory. The other components of the bloch vector are $r_2 = -\sin^2 \xi \cos \beta$ and $r_7 = \sin^2 \xi \sin \beta$ with $\xi = \xi_0 \sin^2(2\pi t/\tau)$; r_4 is used to cancel the initial-final state coupling, which is determined by the equation $\Omega_c^i(r_4) = 0$.

In FIGS. 5 (a) and (b), we plot the control field Ω_p and the population on $|^1E\rangle$ as a function of the dimensionless time t/τ . The red dash lines are the results given by the mixed-state protocol, and the green dot-dash lines and the blue solid lines are the numerical results given by the pure-state protocol with $\gamma_0 = 0.1$ and $\gamma_0 = 0.01$ respectively. As shown in FIG.5 (a), the mixed-state protocol only requires finite strength of the control field Ω_p^i , even if the population on $|^1E\rangle$ is zero. But, for the PIE scheme, the strength of Ω_p tends to infinity when the population on $|^1E\rangle$ goes to zero at $t/\tau = 1$. The finite control field strength is the contribution from designable r_2 and r_7 . For $t/\tau = 1$, it can be obtained that the final state satisfies $r_3 = 0$, $r_8 = -1$ and $r_4 = 0$, and the time derivative of these components of the general Bloch vector are zeros. Then, we can obtain the control field Ω_p^i as a function of r_2 and r_7 from Eq.(D1), which reads

$$\Omega_p^i = -\frac{2\sqrt{3}\partial_t r_7 r_2 - \sqrt{3}\partial_t r_2 r_7 + 2\sqrt{3}\Gamma r_2 r_7}{2r_2(-r_2^2 + r_7^2 + 3)}. \quad (26)$$

This equation illustrates that, even if $|^1E\rangle$ is unpopulated, we can still obtain a finite control field by selecting proper relation between r_2 and r_7 . Substituting the concrete parameterized r_2 and r_7 into Eq.(26), we finally obtain $\Omega_p^i(\tau) = 0$. To illustrate this clearly, we further plot the ratio between the control fields for the mixed-state protocol $\Omega_p^i(t)$ and the pure-state protocol $\Omega_p(t)$ with $\gamma_0 = 0.01$ in FIG. 5 (c). When $t/\tau \rightarrow 0$ and $t/\tau \rightarrow 1$ (the minimal population on $|^1E\rangle$ for the pure-state protocol), the ratio goes to infinity, which verifies that the mixed-state protocol does not require a extremely strong control field in the control process. As shown in FIG.5 (d), the MIE scheme also presents a better transfer efficiency than the pure-state inverse engineering scheme.

V. CONCLUSION

To achieve feasible control of open quantum systems with high-accuracy, high-controllability, and high-speed, we propose a fast and robust control scheme. After presenting the STAs based on dynamical invariants of open quantum system, we apply STAs of open quantum systems to accelerate the adiabatic steady process. As a result, with the same form as the reference Liouvillian, the control Liouvillian can drive the open quantum system from an initial steady state into a target steady state

along a designed trajectory with desired fidelity and pulse length. We highlight the high-controllability of the trajectory, which leads to robustness of control protocols to some particular noises and eliminates untunable control manners.

Our scheme opens several promising avenues for further developments. Theoretically, it would be interesting to explore possible speed-limits and trade-off relations for the open quantum systems [33, 34]. Experimentally, due to the feasible of the MIE protocol, the present protocol can be realized in various systems, such as cavity quantum electrodynamical systems[35], superconducting circuits [27], nitrogen-vacancy centers [26] and spin-chains[36].

This work is supported by National Natural Science Foundation of China (NSFC) under Grants No. 12075050 and 11775048.

Appendix A: The General Solution of Eq.(1)

The dynamical invariants $\hat{\mathcal{I}}(t)$ are defined as superoperators which satisfy the dynamical equation

$$\partial_t \hat{\mathcal{I}}(t) - [\hat{\mathcal{L}}_c(t), \hat{\mathcal{I}}(t)] = 0, \quad (A1)$$

where $\hat{\mathcal{L}}(t)$ is the control Liouvillian superoperator. Generally speaking, the superoperator $\hat{\mathcal{I}}(t)$ is non-Hermitian. We can introduce a right basis $\{|D_\alpha^{(i)}\rangle\}$ and left basis $\{\langle\langle E_\alpha^{(i)}|\}$ in Hilbert-Schmidt space based on the Jordan canonical form. The left and right basis always satisfy

$$\begin{aligned} \hat{\mathcal{I}}|D_\alpha^{(i)}\rangle &= \lambda_\alpha|D_\alpha^{(i)}\rangle + |D_\alpha^{(i-1)}\rangle, \\ \langle\langle E_\alpha^{(i)}|\hat{\mathcal{I}} &= \lambda_\alpha\langle\langle E_\alpha^{(i)}| + \langle\langle E_\alpha^{(i+1)}|, \end{aligned} \quad (A2)$$

where

$$|D_\alpha^{(-1)}\rangle \equiv 0, \quad (A3)$$

$$\langle\langle E_\alpha^{(n_\alpha)}| \equiv 0, \quad (A4)$$

with $i = 0, 1, \dots, n_\alpha - 1$ (n_α is the dimension of the block α). Here we assume that all of eigenvalues are nondegenerate, i.e., $\lambda_\alpha \neq \lambda_\beta$ for $\forall \alpha \neq \beta$. Moreover, the left and right bases satisfy the orthonormality condition

$$\langle\langle E_\alpha^{(i)}|D_\beta^{(j)}\rangle\rangle = \delta_{\alpha\beta}\delta_{ij}$$

The right and left basis $|D_\alpha^{(0)}\rangle$ and $\langle\langle E_\alpha^{(n_\alpha-1)}|$ are the right and left eigenvector of $\hat{\mathcal{I}}(t)$ with the eigenvalue λ_α . Taking the first derivative of Eq.(B4) with respect to time, we have

$$\begin{aligned} \partial_t \hat{\mathcal{I}}|D_\alpha^{(i)}\rangle + \hat{\mathcal{I}}|\partial_t D_\alpha^{(i)}\rangle &= \partial_t \lambda_\alpha|D_\alpha^{(i)}\rangle \\ &+ \lambda_\alpha|\partial_t D_\alpha^{(i)}\rangle + |\partial_t D_\alpha^{(i-1)}\rangle. \end{aligned} \quad (A5)$$

Multiplying above equation and $\langle\langle E_\beta^{(j)}|$ yields

$$\begin{aligned} \langle\langle E_\beta^{(j)}|\partial_t \hat{\mathcal{I}}|D_\alpha^{(i)}\rangle\rangle &= \partial_t \lambda_\alpha \delta_{\alpha\beta} \delta_{ij} \\ &+ (\lambda_\alpha - \lambda_\beta)\langle\langle E_\beta^{(j)}|\partial_t D_\alpha^{(i)}\rangle\rangle + \langle\langle E_\beta^{(j)}|\partial_t D_\alpha^{(i-1)}\rangle\rangle \\ &- \langle\langle E_\beta^{(j+1)}|\partial_t D_\alpha^{(i)}\rangle\rangle. \end{aligned} \quad (A6)$$

Substituting Eq.(A1) into the last equation, we obtain

$$\begin{aligned} \partial_t \lambda_\alpha \delta_{\alpha\beta} \delta_{ij} &= (\lambda_\alpha - \lambda_\beta) \langle \langle E_\beta^{(j)} | \hat{O} | D_\alpha^{(i)} \rangle \rangle \\ &+ \langle \langle E_\beta^{(j)} | \hat{O} | D_\alpha^{(i-1)} \rangle \rangle - \langle \langle E_\beta^{(j+1)} | \hat{O} | D_\alpha^{(i)} \rangle \rangle \end{aligned} \quad (\text{A7})$$

where $\hat{O} \equiv \hat{\mathcal{L}}_c - \partial_t$.

For $\alpha \neq \beta$, the above equation yields

$$\begin{aligned} (\lambda_\alpha - \lambda_\beta) \langle \langle E_\beta^{(j)} | \hat{O} | D_\alpha^{(i)} \rangle \rangle + \langle \langle E_\beta^{(j)} | \hat{O} | D_\alpha^{(i-1)} \rangle \rangle \\ - \langle \langle E_\beta^{(j+1)} | \hat{O} | D_\alpha^{(i)} \rangle \rangle = 0, \end{aligned} \quad (\text{A8})$$

In the following, we illustrate that $\langle \langle E_\beta^{(j)} | \hat{O} | D_\alpha^{(i)} \rangle \rangle = 0$ for $\forall i, j$. Firstly, we notice that above equation is a recurrence equation about the indexes i and j . Setting $i = 0$ and $j = n_\beta - 1$, we obtain

$$\langle \langle E_\beta^{(n_\beta-1)} | \hat{O} | D_\alpha^{(0)} \rangle \rangle = 0, \quad (\text{A9})$$

where Eqs. (A3) and (A4) are used. Then, using the recurrence equation Eq.(A8) again and considering $i = 1$ and $j = n_\beta - 1$, it results in

$$(\lambda_\alpha - \lambda_\beta) \langle \langle E_\beta^{(n_\beta-1)} | \hat{O} | D_\alpha^{(1)} \rangle \rangle + \langle \langle E_\beta^{(n_\beta-1)} | \hat{O} | D_\alpha^{(0)} \rangle \rangle = 0,$$

Placing Eq.(A9) into above equation, we have

$$\langle \langle E_\beta^{(n_\beta-1)} | \hat{O} | D_\alpha^{(1)} \rangle \rangle = 0, \quad (\text{A10})$$

Repeating this procedure and checking every index $i = 1, \dots, n_\alpha - 1$, we conclude that the follow relations are insured,

$$\langle \langle E_\beta^{(n_\beta-1)} | \hat{O} | D_\alpha^{(i)} \rangle \rangle = 0, \forall i = 0, \dots, n_\alpha - 1. \quad (\text{A11})$$

Secondly, we check $\langle \langle E_\beta^{(j)} | \hat{O} | D_\alpha^{(0)} \rangle \rangle$ by the same procedure as before. Setting $j = n_\beta - 2$, Eq.(A8) is turning into

$$\begin{aligned} (\lambda_\alpha - \lambda_\beta) \langle \langle E_\beta^{(n_\beta-2)} | \hat{O} | D_\alpha^{(0)} \rangle \rangle + \langle \langle E_\beta^{(n_\beta-2)} | \hat{O} | D_\alpha^{(-1)} \rangle \rangle \\ - \langle \langle E_\beta^{(n_\beta-1)} | \hat{O} | D_\alpha^{(0)} \rangle \rangle = 0. \end{aligned}$$

Due to the relation Eqs. (A3) and (A9), we immediately have

$$\langle \langle E_\beta^{(n_\beta-2)} | \hat{O} | D_\alpha^{(0)} \rangle \rangle = 0.$$

Thus, reducing the index j step by step and check all terms by Eq.(A8), it can be concluded that

$$\langle \langle E_\beta^{(j)} | \hat{O} | D_\alpha^{(0)} \rangle \rangle = 0. \quad (\text{A12})$$

Equipping with Eqs. (A11) and (A12), we check the other indexes i and j by the recurrence equation. For instance, setting $i = 1$ and $j = n_\beta - 2$, we have

$$\begin{aligned} (\lambda_\alpha - \lambda_\beta) \langle \langle E_\beta^{(n_\beta-2)} | \hat{O} | D_\alpha^{(1)} \rangle \rangle + \langle \langle E_\beta^{(n_\beta-2)} | \hat{O} | D_\alpha^{(0)} \rangle \rangle \\ - \langle \langle E_\beta^{(n_\beta-1)} | \hat{O} | D_\alpha^{(1)} \rangle \rangle = 0, \end{aligned}$$

It yields

$$\langle \langle E_\beta^{(n_\beta-2)} | \hat{O} | D_\alpha^{(1)} \rangle \rangle = 0, \quad (\text{A13})$$

by using Eqs. (A11) and (A12). As a result, when all of the indexes i and j are iterated, we conclude that

$$\langle \langle E_\beta^{(j)} | \hat{O} | D_\alpha^{(i)} \rangle \rangle = 0, \forall i, j, \quad (\text{A14})$$

for $\lambda_\alpha \neq \lambda_\beta$ for $\forall \alpha \neq \beta$.

In case of $\alpha = \beta$, Eq.(A7) can be written as

$$\partial_t \lambda_\alpha \delta_{ij} = \langle \langle E_\alpha^{(j)} | \hat{O} | D_\alpha^{(i-1)} \rangle \rangle - \langle \langle E_\alpha^{(j+1)} | \hat{O} | D_\alpha^{(i)} \rangle \rangle,$$

Therefore, we can obtain the dynamical equation of the eigenvalues by taking sum over all indexes i and j of the Jordan block α ,

$$\partial_t \lambda_\alpha = \frac{1}{n_\alpha} \sum_{i,j=0}^{n_\alpha-1} \left(\langle \langle E_\alpha^{(j)} | \hat{O} | D_\alpha^{(i-1)} \rangle \rangle - \langle \langle E_\alpha^{(j+1)} | \hat{O} | D_\alpha^{(i)} \rangle \rangle \right),$$

If $i \neq j$, we find that

$$\langle \langle E_\alpha^{(j)} | \hat{O} | D_\alpha^{(i-1)} \rangle \rangle = \langle \langle E_\alpha^{(j+1)} | \hat{O} | D_\alpha^{(i)} \rangle \rangle,$$

Thus, we can write the dynamical equation of eigenvalues as

$$\begin{aligned} \partial_t \lambda_\alpha &= \\ &\frac{1}{n_\alpha} \left(\sum_{i=0}^{n_\alpha-1} \langle \langle E_\alpha^{(i)} | \hat{O} | D_\alpha^{(i-1)} \rangle \rangle - \sum_{j=0}^{n_\alpha-1} \langle \langle E_\alpha^{(j+1)} | \hat{O} | D_\alpha^{(j)} \rangle \rangle \right), \end{aligned}$$

Replacing the index j by $k = j + 1$, it yields

$$\begin{aligned} \partial_t \lambda_\alpha &= \\ &\frac{1}{n_\alpha} \left(\sum_{i=0}^{n_\alpha-1} \langle \langle E_\alpha^{(i)} | \hat{O} | D_\alpha^{(i-1)} \rangle \rangle - \sum_{k=1}^{n_\alpha} \langle \langle E_\alpha^{(k)} | \hat{O} | D_\alpha^{(k-1)} \rangle \rangle \right) \\ &= \frac{1}{n_\alpha} \left(\langle \langle E_\alpha^{(0)} | \hat{O} | D_\alpha^{(-1)} \rangle \rangle - \langle \langle E_\alpha^{(n_\alpha)} | \hat{O} | D_\alpha^{(n_\alpha-1)} \rangle \rangle \right), \end{aligned}$$

Then, by considering Eqs. (A3) and (A4), we finally obtain

$$\partial_t \lambda_\alpha = 0, \quad (\text{A15})$$

which implies that the dynamical invariants have indeed time-independent eigenvalues.

Let us consider now the solution of the master equation with the Liouvillian $\hat{\mathcal{L}}_c(t)$, i.e.,

$$\partial_t |\rho(t)\rangle\rangle = \hat{\mathcal{L}}_c(t) |\rho(t)\rangle\rangle. \quad (\text{A16})$$

We expand the density matrix vector by the left basis vectors of the dynamical invariant $\hat{\mathcal{I}}(t)$,

$$|\rho(t)\rangle\rangle = \sum_{\alpha=0}^{m-1} c_\alpha(t) |\Phi_\alpha(t)\rangle\rangle, \quad (\text{A17})$$

with

$$|\Phi_\alpha(t)\rangle\rangle = \sum_{i=0}^{n_\alpha-1} b_i^\alpha(t) |D_\alpha^{(i)}(t)\rangle\rangle, \quad (\text{A18})$$

where m is the number of Jordan blocks. Inserting Eq.(A17) into Eq.(A16), it yields

$$\begin{aligned} \sum_{\alpha=0}^{m-1} \partial_t c_{\alpha}(t) |\Phi_{\alpha}(t)\rangle \rangle + \sum_{\alpha=0}^{m-1} c_{\alpha}(t) \partial_t |\Phi_{\alpha}(t)\rangle \rangle \\ = \sum_{\alpha=0}^{m-1} c_{\alpha}(t) \hat{\mathcal{L}}_c(t) |\Phi_{\alpha}(t)\rangle \rangle. \end{aligned} \quad (\text{A19})$$

Here we define a left vector $\langle\langle \Psi_{\beta}(t) |$ of the Jordan block β , which satisfy $\langle\langle \Psi_{\beta}(t) | \Phi_{\alpha}(t)\rangle \rangle = \delta_{\alpha\beta}$. This left vector can be expanded by the left basis vectors of the Jordan block β , i.e., $\langle\langle \Psi_{\beta}(t) | = \sum_{j=0}^{n_{\beta}-1} a_j^{\beta}(t) \langle\langle E_{\beta}^{(j)}(t) |$. Projecting Eq.(A19) in $\langle\langle \Psi_{\beta}(t) |$, we obtain

$$\partial_t c_{\beta}(t) = \sum_{\alpha=0}^{m-1} c_{\alpha}(t) \langle\langle \Psi_{\beta}(t) | \hat{O}(t) | \Phi_{\alpha}(t)\rangle \rangle, \quad (\text{A20})$$

with

$$\langle\langle \Psi_{\beta}(t) | \hat{O}(t) | \Phi_{\alpha}(t)\rangle \rangle = \sum_{i,j} a_j^{\beta}(t) b_i^{\alpha}(t) \langle\langle E_{\beta}^{(j)} | \hat{O} | D_{\alpha}^{(i)}\rangle \rangle.$$

By making use of Eq.(A14), we have

$$\partial_t c_{\beta}(t) = c_{\beta}(t) \langle\langle \Psi_{\beta}(t) | \hat{O}(t) | \Phi_{\beta}(t)\rangle \rangle. \quad (\text{A21})$$

This results in a formal solution of the density matrix vector

$$|\rho(t)\rangle \rangle = \sum_{\alpha=0}^{m-1} c_{\alpha}(0) |\tilde{\Phi}_{\alpha}(t)\rangle \rangle, \quad (\text{A22})$$

with “dynamical modes” $|\tilde{\Phi}_{\alpha}(t)\rangle \rangle = \exp(\eta_{\alpha}(t)) |\Phi_{\alpha}(t)\rangle \rangle$, where the phases are defined as

$$\eta_{\alpha}(t) = \int_0^t d\tau \langle\langle \Psi_{\alpha}(\tau) | \hat{O}(\tau) | \Phi_{\alpha}(\tau)\rangle \rangle. \quad (\text{A23})$$

In fact, we do not obtain a complete solution of the master equation Eq.(A16), since the coefficients in $|\phi_{\alpha}(t)\rangle \rangle$ have not been determined. This will be an interesting and open question for further investigation. But the formal solution in Eq.(A22) is enough to establish the shortcuts to adiabaticity of open quantum systems, since the adiabatic theorem of open quantum systems just requires that the transition between different Jordan blocks are forbidden [10]. Putting undetermined coefficients in $|\phi_{\alpha}(t)\rangle \rangle$ aside, we only need to ensure the quantum state in the same Jordan block of $\hat{\mathcal{L}}_c(t)$ at the beginning and end of control process.

Appendix B: Comparison with the Transitionless Driving Scheme of Open Quantum Systems

In the following, we present a proof that our scheme is as general as, in some cases it is beyond, the G. Vacanti’s method [15].

For the reference Liouvillian superoperator $\hat{\mathcal{L}}_0(t)$, it is always possible to find a similarity transformation $C(t)$ such that $\hat{\mathcal{L}}_0(t)$ is written in the canonical Jordan form

$$\hat{\mathcal{L}}_J(t) = C^{-1}(t) \hat{\mathcal{L}}_0(t) C(t) = \text{diag}[J_1(t), \dots, J_N(t)] \quad (\text{B1})$$

where $J_{\alpha}(t)$ represents the Jordan block (of dimension n_{α}) corresponding to the eigenvalue $\zeta_{\alpha}(t)$ of $\hat{\mathcal{L}}_0(t)$. The number N of Jordan blocks is equal to the number of linear independent eigenvectors of $\hat{\mathcal{L}}_0(t)$ and the similarity transformation is given by

$$C(t) = \sum_{\alpha=1}^N \sum_{i=1}^{n_{\alpha}} |D_{\alpha}^{(i)}(t)\rangle \rangle \langle\langle \sigma_{\alpha}^{(i)}|,$$

where $\{|D_{\alpha}^{(i)}(t)\rangle \rangle\}$ is a right instantaneous quasi-eigenbases of $\hat{\mathcal{L}}_0(t)$ associated with the eigenvalues $\{\zeta_{\alpha}(t)\}$ which satisfies

$$\hat{\mathcal{L}}_0 |D_{\alpha}^{(i)}\rangle \rangle = \zeta_{\alpha} |D_{\alpha}^{(i)}\rangle \rangle + |D_{\alpha}^{(i-1)}\rangle \rangle.$$

And $\{|\sigma_{\alpha}^{(i)}\rangle\}$ is a set of time-independent bases which is used to calculate the matrix form of $\hat{\mathcal{L}}_0(t)$.

Here we construct a dynamical invariant superoperator $\hat{\mathcal{I}}(t)$ which have same Jordan blocks structure. In other words, $\hat{\mathcal{I}}(t)$ can be diagonal by the same similarity transformation $C(t)$, i.e.,

$$\hat{\mathcal{I}}_J = C^{-1}(t) \hat{\mathcal{I}}(t) C(t) = \text{diag}[I_1, \dots, I_N], \quad (\text{B2})$$

where I_{α} is the Jordan block (of dimension n_{α}) corresponding to the eigenvalue λ_{α} of $\hat{\mathcal{I}}(t)$. The eigenvalues $\{\lambda_{\alpha}\}$ are time-independent. In fact, we choose a dynamical invariant with the same Jordan blocks structure is equivalent to choose the trajectory of the mixed-state inverse engineering as the adiabatic trajectory. Therefore, $\hat{\mathcal{L}}_0(t)$ and $\hat{\mathcal{I}}(t)$ share common quasi-eigenvectors $|D_{\alpha}^{(i)}(t)\rangle \rangle$, i.e.,

$$\hat{\mathcal{I}} |D_{\alpha}^{(i)}\rangle \rangle = \lambda_{\alpha} |D_{\alpha}^{(i)}\rangle \rangle + |D_{\alpha}^{(i-1)}\rangle \rangle.$$

The dynamical invariants $\hat{\mathcal{I}}(t)$ satisfy the dynamical equation Eq.(A1) Following the G. Vacanti method, we set that the control Liouvillian superoperator can be written as $\hat{\mathcal{L}}(t) = \hat{\mathcal{L}}_0(t) + \hat{\mathcal{L}}_c(t)$, where $\hat{\mathcal{L}}_c(t)$ is the counterdiabatic superoperator. Substituting Eq.(B2) into Eq.(A1), it yields

$$\partial_t \left(C \hat{\mathcal{I}}_J C^{-1} \right) = [C \hat{\mathcal{L}}_J C^{-1} + \hat{\mathcal{L}}_c, C \hat{\mathcal{I}}_J C^{-1}] \quad (\text{B3})$$

where Eq.(B1) has been used. Considering that $\hat{\mathcal{I}}_J$ is time-independent and taking the same similarity transformation $C(t)$ on above equation, we obtain

$$\left[C^{-1} \partial_t C, \hat{\mathcal{I}}_J \right] = \left[\hat{\mathcal{L}}_J, \hat{\mathcal{I}}_J \right] + \left[C^{-1} \hat{\mathcal{L}}_c C, \hat{\mathcal{I}}_J \right]. \quad (\text{B4})$$

in which the fact $C^{-1} \partial_t C = -\partial_t C^{-1} C$ are considered. Since $\hat{\mathcal{I}}(t)$ and $\hat{\mathcal{L}}_0(t)$ have same Jordan blocks structure, we have $[\hat{\mathcal{L}}_J, \hat{\mathcal{I}}_J] = 0$. It is not difficult to see that, if

$\hat{\mathcal{L}}'_c \equiv C^{-1} \hat{\mathcal{L}}_c C = C^{-1} \partial_t C$, Eq.(B4) holds. We expand $\hat{\mathcal{L}}'_c$ by the bases $\{|\sigma_\alpha^{(i)}\rangle\}$, and separate it into two parts, $\hat{\mathcal{L}}'_c = \hat{\mathcal{L}}'_J + \hat{\mathcal{L}}'_{nd}$, where

$$\begin{aligned}\hat{\mathcal{L}}'_J &= \sum_{\alpha, i, j} C_\alpha^{i, j} |\sigma_\alpha^{(i)}\rangle \langle \langle \sigma_\alpha^{(j)}|, \\ \hat{\mathcal{L}}'_{nd} &= \sum_{\alpha \neq \beta, i, j} C_{\alpha, \beta}^{i, j} |\sigma_\alpha^{(i)}\rangle \langle \langle \sigma_\beta^{(j)}|,\end{aligned}$$

with $C_{\alpha, \beta}^{i, j} = \langle \langle \sigma_\alpha^{(j)} | C^{-1} \partial_t C | \sigma_\beta^{(i)} \rangle \rangle$. The superoperator $\hat{\mathcal{L}}'_{nd}$ is used to forbid the transitions from J_α to J_β . Therefore, the counterdiabatic superoperator which really required for STAs is

$$\hat{\mathcal{L}}_{\text{tqd}}(t) = C(t) \hat{\mathcal{L}}'_{nd}(t) C^{-1}(t). \quad (\text{B5})$$

Comparing Eq.(B5) with Eq. (15) in Ref.[15], we immediately find that $\hat{\mathcal{L}}_{\text{tqd}}(t)$ is the very counterdiabatic superoperator given by G. Vacanti and his co-authors [15].

Above simple proof illustrates that, if the trajectory of the general STAs based on the invariant theory of open quantum systems is chosen as the adiabatic trajectory, our method is coincident with the transitionless quantum driving method proposed in Ref.[15]. However, the adiabatic trajectory is not the only choice of the trajectories in our scheme. There are many trajectories can be used to inversely engineer the open quantum system. As shown by the example in Sec. III B, proper trajectories can always produce reasonable and applicable control protocols, which helps us to overcome the difficulties met

in the control of microscopic or/and mesoscopic systems. Hence, the mixed-state inverse engineering is more general than the transitionless quantum driving method of open quantum systems proposed by G. Vacanti [15].

The main difficulty in the G. Vacanti's method is how to realize the counterdiabatic superoperator into a practical control. The MIE scheme solves those problems by selecting proper trajectories. According to the symmetry of the open quantum systems, we can choose flexibly the form of the control Liouvillian, this make the proposal widely applicable in the control of open quantum systems.

Appendix C: The Instantaneous Steady State of $\hat{\mathcal{L}}_0(t)$

We use the “bra-ket” notation for the superoperator to rewrite the master equation Eq.(12), and reshape the density matrix into a 1×9 complex vector. The density matrix vector can be written as

$$|\rho\rangle\rangle = (\rho_{-1-1}, \rho_{-12}, \rho_{-11}, \rho_{2-1}, \rho_{22}, \rho_{21}, \rho_{1-1}, \rho_{12}, \rho_{11})^T$$

with $\rho_{ij} = \langle i | \hat{\rho} | j \rangle$. In order to present an analytic result, we assume that $\Gamma_{-1} = \Gamma_{+1} \equiv \Gamma$ and $\omega_{2 \rightarrow -1} = \omega_{2 \rightarrow +1} \equiv \omega_0$. At room temperature ($T=300$ K), the mean excitation number is $N = 1.9 \times 10^{-33}$. For practice application, we choose the instantaneous steady state of the reference Liouvillian $\hat{\mathcal{L}}_0$ as the trajectory of inverse engineering, in this case the dephasing is the key obstacle for the performance of the protocol. The reference Liouvillian superoperator $\hat{\mathcal{L}}_0$ can be expressed as a 9×9 matrix,

$$\hat{\mathcal{L}}_0 = \hbar \Gamma \begin{pmatrix} -2N & i\Omega_p/\Gamma & 0 & -i\Omega_p/\Gamma & 2(N+1) & 0 & 0 & 0 & 0 \\ i\Omega_p/\Gamma & -(3N+2) & i\Omega_s/\Gamma & 0 & -i\Omega_p/\Gamma & 0 & 0 & 0 & 0 \\ 0 & i\Omega_s/\Gamma & -2N & 0 & 0 & -i\Omega_p/\Gamma & 0 & 0 & 0 \\ -i\Omega_p/\Gamma & 0 & 0 & -(3N+2) & i\Omega_p/\Gamma & 0 & -i\Omega_s/\Gamma & 0 & 0 \\ 2N & -i\Omega_p/\Gamma & 0 & i\Omega_p/\Gamma & -4(N+1) & i\Omega_s/\Gamma & 0 & -i\Omega_s/\Gamma & 2N \\ 0 & 0 & -i\Omega_p/\Gamma & 0 & i\Omega_s/\Gamma & -(3N+2) & 0 & 0 & -i\Omega_s/\Gamma \\ 0 & 0 & 0 & -i\Omega_s/\Gamma & 0 & 0 & -2N & i\Omega_p/\Gamma & 0 \\ 0 & 0 & 0 & 0 & -i\Omega_s/\Gamma & 0 & i\Omega_p/\Gamma & -(3N+2) & i\Omega_s/\Gamma \\ 0 & 0 & 0 & 0 & 2(N+1) & -i\Omega_s/\Gamma & 0 & i\Omega_s/\Gamma & -2N \end{pmatrix}.$$

The steady state is obtained immediately by considering $\hat{\mathcal{L}}_0|\rho_0\rangle\rangle = 0$,

$$|\rho_0\rangle\rangle = \frac{1}{z} \begin{pmatrix} (3N^2 + 2N)(N+1)\Gamma^2 + N\Omega^2 + \Omega_p^2 \\ -iN\Gamma\Omega_p \\ -\Omega_p\Omega_s \\ iN\Gamma\Omega_p \\ N^2(3N+2)\Gamma^2 + N\Omega^2 \\ iN\Gamma\Omega_s \\ -\Omega_p\Omega_s \\ -iN\Gamma\Omega_s \\ (3N^2 + 2N)(N+1)\Gamma^2 + N\Omega^2 + \Omega_s^2 \end{pmatrix}. \quad (\text{C1})$$

with the normalized factor

$$z = (3N+1)\Omega^2 + N\Gamma^2(3N+2)^2.$$

For $N = 0$, the instantaneous steady state is the dark state of the Hamiltonian Eq.(10), i.e. $|\rho_0\rangle\rangle = (\cos^2 \theta, 0, \sin \theta \cos \theta, 0, 0, 0, \sin \theta \cos \theta, 0, \sin^2 \theta)^T$.

We parameterize the adiabatic trajectory given by the instantaneous steady state of $\hat{\mathcal{L}}_0$ via the generalized Bloch vector $\{r_k\}_{k=1}^8$, which expands the density matrix of the three-level system as follows,

$$\rho(t) = \frac{1}{3} \left(\mathbf{I} + \sqrt{3} \sum_{k=1}^8 r_k(t) T_k \right), \quad (\text{C2})$$

where \mathbf{I} is a 3×3 identity matrix, and T_k denotes the regular Gellmann matrix

$$\begin{aligned} T_1 &= \begin{pmatrix} 0 & 1 & 0 \\ 1 & 0 & 0 \\ 0 & 0 & 0 \end{pmatrix}, \quad T_2 = \begin{pmatrix} 0 & -i & 0 \\ i & 0 & 0 \\ 0 & 0 & 0 \end{pmatrix}, \quad T_3 = \begin{pmatrix} 1 & 0 & 0 \\ 0 & -1 & 0 \\ 0 & 0 & 0 \end{pmatrix}, \quad T_4 = \begin{pmatrix} 0 & 0 & 1 \\ 0 & 0 & 0 \\ 1 & 0 & 0 \end{pmatrix}, \\ T_5 &= \begin{pmatrix} 0 & 0 & -i \\ 0 & 0 & 0 \\ i & 0 & 0 \end{pmatrix}, \quad T_6 = \begin{pmatrix} 0 & 0 & 0 \\ 0 & 0 & 1 \\ 0 & 1 & 0 \end{pmatrix}, \quad T_7 = \begin{pmatrix} 0 & 0 & 0 \\ 0 & 0 & -i \\ 0 & i & 0 \end{pmatrix}, \quad T_8 = \frac{1}{\sqrt{3}} \begin{pmatrix} 1 & 0 & 0 \\ 0 & 1 & 0 \\ 0 & 0 & -2 \end{pmatrix}. \end{aligned} \quad (\text{C3})$$

These $\{T_\mu\}$ span all traceless Hermitian matrices of the Lie algebra $\text{su}(3)$. Thus, the Bloch vectors corresponding to the instantaneous steady state Eq.(C1) are

$$\begin{aligned} r_2 &= \sqrt{3} N \Gamma \Omega_p / z, \\ r_3 &= \sqrt{3} ((3N^2 + 2N) \Gamma^2 + \Omega_s^2) / (2z), \\ r_4 &= -\sqrt{3} \Omega_p \Omega_s / z, \\ r_7 &= -\sqrt{3} N \Gamma \Omega_s / z, \\ r_8 &= -((3N^2 + 2N) \Gamma^2 + 2 \Omega_p^2 - \Omega_s^2) / (2z), \end{aligned} \quad (\text{C4})$$

and the other components are zeros. Correspondingly, the dynamical invariants can be parameterized by the Bloch vector according to our proposal (see Eq.(8)),

$$\hat{\mathcal{I}}(t) = \frac{\sqrt{3}}{3} \Omega_I \begin{pmatrix} \left(r_3 + \frac{\sqrt{3}r_8}{3}\right) + \frac{\sqrt{3}}{3} & 0 & 0 & 0 & \left(r_3 + \frac{\sqrt{3}r_8}{3}\right) + \frac{\sqrt{3}}{3} & 0 & 0 & 0 & \left(r_3 + \frac{\sqrt{3}r_8}{3}\right) + \frac{\sqrt{3}}{3} \\ i r_2 & 0 & 0 & 0 & i r_2 & 0 & 0 & 0 & i r_2 \\ r_4 & 0 & 0 & 0 & r_4 & 0 & 0 & 0 & r_4 \\ -i r_2 & 0 & 0 & 0 & -i r_2 & 0 & 0 & 0 & -i r_2 \\ \frac{\sqrt{3}}{3} - \left(r_3 - \frac{\sqrt{3}r_8}{3}\right) & 0 & 0 & 0 & \frac{\sqrt{3}}{3} - \left(r_3 - \frac{\sqrt{3}r_8}{3}\right) & 0 & 0 & 0 & \frac{\sqrt{3}}{3} - \left(r_3 - \frac{\sqrt{3}r_8}{3}\right) \\ i r_7 & 0 & 0 & 0 & i r_7 & 0 & 0 & 0 & i r_7 \\ r_4 & 0 & 0 & 0 & r_4 & 0 & 0 & 0 & r_4 \\ -i r_7 & 0 & 0 & 0 & -i r_7 & 0 & 0 & 0 & -i r_7 \\ \frac{\sqrt{3}}{3} - \frac{2\sqrt{3}r_8}{3} & 0 & 0 & 0 & \frac{\sqrt{3}}{3} - \frac{2\sqrt{3}r_8}{3} & 0 & 0 & 0 & \frac{\sqrt{3}}{3} - \frac{2\sqrt{3}r_8}{3} \end{pmatrix} \quad (\text{C5})$$

where Ω_I is an arbitrary nonzero constant.

Appendix D: The Control Parameters in the Control Liouvillian

Considering the dynamical equation of the dynamical invariants Eq.(A1), we can determine all of control parameters in the control Liouvillian $\hat{\mathcal{L}}_c$,

$$\Omega_s^i = n_s/d, \quad \Omega_p^i = n_p/d, \quad \Omega_c^i = n_c/d, \quad N_{-1}^i = n_{-1}/d, \quad N_{+1}^i = n_{+1}/d, \quad (\text{D1})$$

in which

$$\begin{aligned} d &= 2\sqrt{3}r_4^4 C_2 + 4\sqrt{3}r_2^4 C_1 + r_2^2 \left(12r_8(r_4^2 + r_7^2) + 12\sqrt{3}(r_3^2 + r_8^2) C_1 \right) \\ &\quad + r_4^2 \left(6r_7^2 C_2 - 8\sqrt{3}r_3 C_1 C_2 \right) + 8r_3^2 C_2 C_1^2 + 4\sqrt{3}r_3 r_7^2 (r_2^2 - 2r_7^2) \\ &\quad - 8r_2 r_4 r_7 \left(\sqrt{3}r_7^2 + 3C_2 C_4 \right) + 8\sqrt{3}r_2^3 r_4 r_7 + 12r_3 r_7^2 \left(r_3 - (\sqrt{3} - 2) r_8 \right) \left((2\sqrt{3} + 3) r_8 + \sqrt{3}r_3 \right), \end{aligned}$$

$$\begin{aligned}
n_s = & 2\sqrt{3}\partial_t r_2 \left(r_4^2 (r_7^2 - C_1 C_2) + 2r_2^2 r_3 C_1 + r_2 r_4 r_7 (C_2 + 4r_3) + 2r_3 C_2 (2r_7^2 + C_1^2) \right) \\
& + \sqrt{3}\partial_t r_3 \left(-2r_2^3 C_1 + 2r_2 (-C_1^2 C_2 - 2r_7^2 (C_2 + r_3)) - r_4 r_7 (4r_2^2 + r_4^2 - r_7^2 + 2\sqrt{3}r_8 C_1) \right) \\
& + \partial_t r_4 \left(-r_7 (4r_3 C_1^2 - 6r_4^2 C_3) - 4\sqrt{3}r_3 r_7 (r_2^2 + 2r_7^2) - 2\sqrt{3}r_2 r_4 (2C_1 C_2 + 3r_7^2) \right) \\
& + 2\sqrt{3}\partial_t r_7 \left(2r_3 r_4 C_1 C_2 - r_4^3 C_2 - (2\sqrt{3}r_2 r_8 - r_4 r_7) (r_2 r_4 + 2r_3 r_7) \right) \\
& + \partial_t r_8 \left(r_2 (2C_1 C_2^2 + 2r_4^2 C_2 + 2r_7^2 (r_3 + C_1)) + 2r_2^3 C_2 + r_4 r_7 (4C_2^2 + 2r_2^2 + r_4^2 + r_7^2 + 2\sqrt{3}r_8 C_1) \right) \\
& + \Gamma r_2^2 \left(14r_4 r_7 + 2r_4 r_7 (C_3 + 3\sqrt{3}r_3) \right) - r_7^3 \left(2r_4 + 2r_4 (C_3 - 6\sqrt{3}r_3) \right) \\
& - \Gamma r_7 \left(r_4^3 (8C_3 - 4) - r_4 (4\sqrt{3}r_3^3 - 44r_3^2 r_8 + 4r_3^2 + 4\sqrt{3}r_3 r_8^2 + 16\sqrt{3}r_3 r_8 - 12r_8^3 - 12r_8^2) \right) \\
& - \Gamma r_2^3 \left(4\sqrt{3}r_8 - 8r_3 + 4r_8 C_2 \right) + \Gamma r_2 r_7^2 \left(16r_3 + 4\sqrt{3}r_8 + 4r_8 C_2 \right) \\
& + \Gamma r_2 r_4^2 \left(8\sqrt{3}r_7^2 + (2 - 6\sqrt{3}r_3 + 14r_8) C_2 \right) - \Gamma r_2 C_1 C_2 \left(4\sqrt{3}r_8 - 8r_3 + 4r_8 C_2 \right),
\end{aligned}$$

$$\begin{aligned}
n_p = & \partial_t r_2 \left(6r_4^3 C_2 - r_4 (12r_3 C_1 C_2 - 6\sqrt{3}r_7^2 C_3) + 6r_2 r_7 (r_4^2 + \sqrt{3}C_1 C_3) + 6r_2^2 r_4 C_1 \right) \\
& + \partial_t r_3 \left(3r_4^2 r_7 C_2 - 6r_2^2 r_7 C_1 - 3r_2 r_4 (r_4^2 + 3r_7^2 - 2C_1 (r_3 + C_2)) + 6r_7 - C_1 \left(r_3 C_2 - \frac{r_7^2}{2} \right) \right) \\
& + 6\partial_t r_4 \left(-2C_1 r_2^3 - 3r_4 r_7 r_2^2 + (-2\sqrt{3}r_8 r_4^2 - C_1 (4r_3^2 + r_7^2)) r_2 - 4r_3 r_4 r_7 C_2 \right) \\
& + \partial_t r_7 \left(r_2^2 (-12C_1 C_2 + 6r_4^2) - 24r_3^2 C_1 C_2 + 12r_3 r_4^2 C_2 + 12r_3 r_7^2 C_1 + 6r_2 r_4 r_7 (3C_1 - 2r_3) \right) \\
& + \partial_t r_8 \left(\sqrt{3}r_4^2 r_7 C_2 - 4\sqrt{3}r_2^2 r_7 C_2 - \sqrt{3}r_2 r_4 (2(r_3 + C_2)^2 - 5r_7^2) - \sqrt{3}r_2 r_4 (2r_2^2 - r_4^2) \right) \\
& + \partial_t r_8 \left(-7\sqrt{3}r_3 r_7 (2r_3^2 - r_7^2) + 2\sqrt{3}r_3 r_8 (r_2 r_4 - 3r_7 r_8) - 3r_7 r_8 (4r_3 - r_7) (4r_3 + r_7) \right) \\
& + \Gamma r_2 \left(2r_7^2 (-2r_3 + 5C_1 + 7\sqrt{3}) - 4\sqrt{3} (r_8 + 1) (4r_3^2 + C_1 C_2) + 36r_3 r_4 (r_3^2 + r_8^2) \right) \\
& + \Gamma \left(-r_7^3 (-4r_8 - 10C_4 + 2\sqrt{3}C_2 C_3) + r_2^2 (2r_7 C_2^2 - 12r_7 (3r_8 - 2r_4^2) + 2r_7 C_2 (2r_3 + \sqrt{3})) \right) \\
& + \Gamma \left(r_2^3 (18r_4 C_1 - 2\sqrt{3}r_4 (2r_8 + 1)) + 4\sqrt{3} (4r_8 + 1) r_2 r_4^3 \right) \\
& - \Gamma r_7 \left(r_4^2 C_2 (2\sqrt{3} - 30r_3 + 2\sqrt{3}r_8) - 4r_3 (C_2 (2r_8 - 5C_4) + r_3 C_2 (5C_3 - 2r_3) - \sqrt{3}r_8 C_1 C_2) \right),
\end{aligned}$$

$$\begin{aligned}
n_c = & \partial_t r_2 \left(6r_2 r_4 (r_7^2 + \sqrt{3}C_1 C_4) + 12r_3 r_7 (r_4^2 + 2r_7^2) - 6r_2^2 r_7 C_1 + 12r_3 r_7 C_1^2 \right) \\
& + \partial_t r_3 \left(r_4 (6r_3 C_1^2 + 3r_7^2 C_2) - 3r_4^3 C_1 - 6r_2^2 r_4 C_1 - r_2 r_7 (3r_4^2 + 9r_7^2 + 6C - 1 (r_3 - C_1)) \right) \\
& + \partial_t r_4 \left(12r_3 r_4^2 C_1 - r_2^2 (12C_1^2 + 18r_7^2) - 24r_3^2 (C_1^2 + 2r_7^2) - 6\sqrt{3}r_2 r_4 r_7 C_4 \right) \\
& + \partial_t r_7 \left(6r_7 (r_2 (r_2 r_4 - 2r_3 r_7) - 2\sqrt{3}r_3 r_4 C_4) + 12r_2^3 C_1 + 6r_2 C_1 (4r_3^2 + r_4^2) \right) \\
& + \partial_t r_8 \left((3r_8 + 3\sqrt{3}r_3) r_4^3 + (3r_7^2 (r_8 + 3\sqrt{3}r_3) + 12r_2^2 r_8 - 6r_3 (r_8 + \sqrt{3}r_3) (r_3 - \sqrt{3}r_8)) r_4 \right) \\
& + \partial_t r_8 \left(r_2 r_7 (6\sqrt{3}r_2^2 + 4\sqrt{3}r_3^2 + \sqrt{3}r_4^2 - 3\sqrt{3}r_7^2) + 6\frac{\sqrt{3}}{3}r_2 r_7 C_4 (r_8 + 2C_3) \right) \\
& + \Gamma \left(r_2^2 (24r_4 r_7^2 - 6r_4 (r_8 - \sqrt{3}r_3) (\sqrt{3}r_3 - 5r_8 + 1)) - 6r_2^3 r_7 (r_3 + \sqrt{3}r_8 - \sqrt{3}) \right) \\
& + \Gamma \left(r_2 ((6C_2 + 6\sqrt{3}) r_7^3 + (r_4^2 (8\sqrt{3}C_4 + 4\sqrt{3}) + 4\sqrt{3} (\sqrt{3}C_1 C_4 + 4r_3^2) + 4\sqrt{3}C_2^2 C_1) r_7) \right) \\
& + \Gamma \left(r_4 r_7^2 (6C_4 + \sqrt{3}C_4 (18r_3 + 2\sqrt{3}r_8)) - 6r_4^3 C_4 (C_4 + 2) + 12r_3 C_1 C_4 r_4 (C_4 - 1) \right),
\end{aligned}$$

$$\begin{aligned}
n_{-1} = & \partial_t r_2 \left(6\sqrt{3}r_4 r_7 (C_1^2 - 3r_2^2 + r_4^2 + 2r_7^2) - 6\sqrt{3}r_2^3 C_1 - \sqrt{3}r_2 (6C_1^2 C_2 - 12r_4^2 C_1 + 12r_7^2 C_2) \right) \\
& + \partial_t r_3 \left(-3\sqrt{3}r_2^2 ((r_4^2 - r_7^2) + 6r_3 C_1) - \sqrt{3}r_7^2 (9r_3 + (\sqrt{3} + 2)r_8) (r_3 - (\sqrt{3} - 2)r_8) \right) \\
& + \partial_t r_3 \left(3\sqrt{3} (3r_7^4 - r_4^4) - 6\sqrt{3}r_3 C_2 C_1^2 + 9r_4^2 C_1 C_3 - 24\sqrt{3}r_2 r_3 r_4 r_7 \right) \\
& + \partial_t r_4 \left(6\sqrt{3}r_7 r_2 (C_1^2 - 3r_4^2 + 2r_7^2 + r_2^2) + \sqrt{3}r_4 (6C_1 (r_4^2 - 2r_2^2) - 12r_3 (C_1^2 + 2r_7^2)) \right) \\
& + \partial_t r_7 \left(\sqrt{3} \left(6r_7 (2\sqrt{3}r_8 r_2^2 - \sqrt{3}r_4^2 C_4) + 6r_2 r_4 (C_1^2 + r_2^2 + r_4^2 - 2r_7^2) \right) \right) \\
& + \partial_t r_8 \left(-r_2^2 (-r_2^2 + 3r_4^2 + 9r_7^2 + 6C_1 (r_3 + C_2)) - 6r_3 C_2 C_1^2 \right) \\
& + \partial_t r_8 \left(3r_4^2 (r_4^2 + 3r_7^2 - C_1^2) + 6r_7^4 - r_7^2 (9r_3 + (\sqrt{3} + 2)r_8) (r_3 - (\sqrt{3} - 2)r_8) - 24\sqrt{3}r_2 r_4 r_7 r_8 \right) \\
& + \Gamma \left(\sqrt{3}r_2^4 (2\sqrt{3}(2r_8 - 1) - 6C_1) - 24r_2 r_4 r_7 (\sqrt{3}(r_2^2 - r_4^2) - \sqrt{3}C_4 + 2\sqrt{3}(r_3^2 - r_8^2)) \right) \\
& + \Gamma \left(-r_2^2 (6C_1^2 (3C_3 + 2r_8 - 1) + \sqrt{3}r_4^2 (2\sqrt{3}(2r_8 - 1) - 18C_1) + 6\sqrt{3}r_7^2 (C_2 + \sqrt{3})) \right) \\
& + \Gamma \left(12(1 - C_1)r_4^4 + (18r_7^2 (C_4 + 1) - 2\sqrt{3}C_1 (4r_3 + C_2) (-2C_1 - \sqrt{3}(r_8 - 1))) r_4^2 \right) \\
& + \Gamma \left(12r_3 C_2 C_1^2 - 12r_7^4 + 18r_7^2 (r_3 + (\sqrt{3} + 2)r_8) (r_3 - (\sqrt{3} - 2)r_8) \right) (1 - C_4),
\end{aligned}$$

$$\begin{aligned}
n_{+1} = & \partial_t r_2 \left(6r_2 (r_7^2 C_3 - r_4^2 C_4) - 2\sqrt{3}r_4 r_7 (-2r_2^2 + 4r_3^2 + r_4^2 + r_7^2) \right) \\
& + \partial_t r_3 \left((r_4^2 + r_7^2) (6r_3 r_8 + \sqrt{3}(r_4^2 - r_7^2)) + 2\sqrt{3} (r_4^2 (r_2 + r_3)^2 - r_7^2 (r_2 - r_3)^2) \right) \\
& + \partial_t r_4 \left(4\sqrt{3} (r_2^2 + 2r_3^2) r_4 C_1 - 4\sqrt{3}r_3 r_4 (r_4^2 - 2r_7^2) - 2\sqrt{3}r_2 r_7 (2r_2^2 + 4r_3^2 - 3r_4^2 + r_7^2) \right) \\
& + \partial_t r_7 \left(-4\sqrt{3}r_2^2 r_7 C_2 - 4\sqrt{3}r_3 r_7 (2r_4^2 - r_7^2 + 2r_3 C_2) - 2\sqrt{3}r_2 r_4 (2r_2^2 + 4r_3^2 + r_4^2 - 3r_7^2) \right) \\
& + \partial_t r_8 \left(4(r_2^2 + C_1 C_2) (r_2^2 + 2r_3^2) - (2r_3^2 + r_4^2 + r_7^2) (r_4^2 + r_7^2) + 8\sqrt{3}r_2 r_4 r_7 r_8 - 6\sqrt{3}r_3 r_8 (r_4^2 - r_7^2) \right) \\
& + \Gamma \left((2r_8 + 6\sqrt{3}r_3 + 2)r_7^4 + 4(r_2^4 - r_4^4) (1 - C_4) \right) \\
& + \Gamma \left(-r_2^2 (6r_4^2 (C_4 + 1) + 2r_7^2 (\sqrt{3}C_2 - 3) - 12(r_3^2 - r_8^2) (1 - C_4)) \right) \\
& + \Gamma \left(4r_3 r_4^2 (r_3 - 3\sqrt{3}r_8) (1 - C_4) - 8\sqrt{3}r_2 r_4 r_7 (r_3^2 - r_8^2 + r_4^2 - r_7^2 + 2\sqrt{3}r_3 r_8 + C_4) \right) \\
& + \Gamma \left(8r_3^2 C_1 C_2 (1 - C_4) - r_7^2 (2r_4^2 (r_8 + 7\sqrt{3}r_3 + 1) + 8r_3^2 (7r_8 + \sqrt{3}r_3 + 1)) \right),
\end{aligned}$$

with $C_1 = r_3 - \sqrt{3}r_8$, $C_2 = r_3 + \sqrt{3}r_8$, $C_3 = \sqrt{3}r_3 + r_8$, $C_4 = \sqrt{3}r_3 - r_8$.

Appendix E: The Bloch vectors of the Trajectory without Initial-to-Final State Couplings

To obtain a reasonable control parameters, the intermediate state $|^1E\rangle$ is allowed to be occupied. Without loss of generality, the trajectory characterized by the Bloch vector is designed as follows:

$$\begin{aligned}
r_3 = & \sqrt{3} ((2N(3N+2)\Gamma^2 + \Omega_p^2 - 6\Omega_p\Omega_s + \Omega_s^2) \\
& + \cos(2\phi(t)) (3(\Omega_p + \Omega_s)^2 + 6N\Gamma^2(3N+2)) \\
& - 4\cos(\phi(t)) (\Omega_p^2 - \Omega_s^2) \\
& + 4\sqrt{2}N\Gamma \sin(\phi(t)) (\Omega_p + \Omega_s) \\
& + 6\sqrt{2}N\Gamma \sin(2\phi(t)) (\Omega_p - \Omega_s)) / (16z).
\end{aligned}$$

$$\begin{aligned}
r_8 = & (- (2N(3N+2)\Gamma^2 + \Omega_p^2 - 6\Omega_p\Omega_s + \Omega_s^2) \\
& - 12\cos(\phi(t)) (\Omega_p^2 - \Omega_s^2) \\
& - \cos(2\phi(t)) (3(\Omega_p + \Omega_s)^2 + 6N\Gamma^2(3N+2)) \\
& + 12\sqrt{2}N\Gamma \sin(\phi(t)) (\Omega_p + \Omega_s) \\
& - 6\sqrt{2}N\Gamma \sin(2\phi(t)) (\Omega_p - \Omega_s)) / (16z),
\end{aligned}$$

in which $\phi(t)$ determines the population on $|^1E\rangle$, i.e.,

$$\begin{aligned}
P_2 = & (2N\Omega^2 + 2N^2\Gamma^2(3N+2) \\
& + \sin(\phi(t))^2 ((\Omega_p + \Omega_s)^2 + 2N\Gamma^2(3N+2)) \\
& - \sqrt{2}N\Gamma \sin(2\phi(t)) (\Omega_p - \Omega_s)) / (2z). \quad (E1)
\end{aligned}$$

r_4 is determined by the implicit differential equation $\Omega_c^i(t) = 0$; r_2 and r_7 are the same as in the adiabatic trajectory (r_2 and r_7 in Eq.(C4)). We consider the adiabatic pulses $\Omega_{p,s}$ like Eq.(11) with

$$\theta(t) = \frac{\pi}{2} \sin\left(\frac{\pi t}{2\tau}\right)^2,$$

and the trajectory with

$$\phi(t) = \frac{\pi}{9} \sin\left(\frac{\pi t}{\tau}\right)^2.$$

Thus, we can determine all of the control parameters numerically.

[1] C. P. Koch, M. Lemeshko, and D. Sugny, Quantum control of molecular rotation, *Rev. Mod. Phys.* **91**, 035005 (2019).

[2] S. Osnaghi, P. Bertet, A. Auffeves, P. Maioli, M. Brune, J. M. Raimond, and S. Haroche, Coherent control of an atomic collision in a cavity, *Phys. Rev. Lett.* **87**, 037902 (2001).

[3] S. Hacohen-Gourgy, L. P. García-Pintos, L. S. Martin, J. Dressel, and I. Siddiqi, Incoherent qubit control using the quantum Zeno effect, *Phys. Rev. Lett.* **120**, 020505 (2018).

[4] P. Král, I. Thanopulos, and M. Shapiro, Colloquium: Coherently controlled adiabatic passage, *Rev. Mod. Phys.* **79**, 53 (2007).

[5] M. V. Berry, Transitionless quantum driving, *J. Phys. A* **42**, 365303 (2009).

[6] X. Chen, I. Lizuain, A. Ruschhaupt, D. Guéry-Odelin, and J. G. Muga, Shortcut to adiabatic passage in two-and three-level atoms, *Phys. Rev. Lett.* **105**, 123003 (2010).

[7] Y. C. Li, X. Chen, Shortcut to adiabatic population transfer in quantum three-level systems: Effective two-level problems and feasible counterdiabatic driving, *Phys. Rev. A* **94**, 063411 (2016).

[8] J. Huneke, G. Platero, and S. Kohler, Steady-state coherent transfer by adiabatic passage, *Phys. Rev. Lett.* **110**, 036802 (2013).

[9] B. B. Zhou, A. Baksic, H. Ribeiro, C. G. Yale, F. J. Heremans, P. C. Jerger, A. Auer, G. Burkard, A. A. Clerk, and D. D. Awschalom, Accelerated quantum control using superadiabatic dynamics in a solid-state lambda system, *Nat. Phys.* **13**, 330 (2017).

[10] M. S. Sarandy and D. A. Lidar, Adiabatic approximation in open quantum systems, *Phys. Rev. A* **71**, 012331 (2005).

[11] L. C. Venuti, T. Albash, D. A. Lidar, and P. Zanardi, Adiabaticity in open quantum systems, *Phys. Rev. A* **93**, 032118 (2016).

[12] S. L. Wu, X. L. Huang, H. Li, and X. X. Yi, Adiabatic evolution of decoherence-free subspaces and its shortcuts, *Phys. Rev. A* **96**, 042104 (2017).

[13] L. Dupays, I. L. Egusquiza, A. del Campo, and A. Chenu, Superadiabatic thermalization of a quantum oscillator by engineered dephasing, *Phys. Rev. Research* **2**, 033178 (2020).

[14] R. Dann, A. Tobalina, and R. Kosloff, Shortcut to equilibration of an open quantum system, *Phys. Rev. Lett.* **122**, 250402 (2019).

[15] G. Vacanti, R. Fazio, S. Montangero, G. M. Palma, M. Paternostro, and V. Vedral, Transitionless quantum driving in open quantum systems, *New J. Phys.* **16**, 053017 (2014).

[16] S. L. Wu, X. L. Huang, and X. X. Yi, Fast trajectory tracking of the steady state of open quantum systems, *Phys. Rev. A* **99**, 042115 (2019).

[17] M. S. Sarandy, E. I. Duzzioni, and M. H. Y. Moussa, Dynamical invariants and nonadiabatic geometric phases in open quantum systems, *Phys. Rev. A* **76**, 052112 (2007).

[18] Xi Chen, E. Torrontegui, and J. G. Muga, Lewis-Riesenfeld invariants and transitionless quantum driving, *Phys. Rev. A* **83**, 062116 (2011).

[19] Xi Chen and J. G. Muga, Engineering of fast population transfer in three-level systems, *Phys. Rev. A* **86**, 033405 (2012).

[20] A. Baksic, H. Ribeiro, and A. A. Clerk, Speeding up adiabatic quantum state transfer by using dressed states, *Phys. Rev. Lett.* **116**, 230503 (2016).

[21] S. Alipour, A. Chenu, A. T. Rezakhani, and A. del Campo, Shortcuts to adiabaticity in driven open quantum systems: Balanced gain and loss and non-Markovian evolution, *Quantum* **4**, 336 (2020).

[22] L. J. Rogers, S. Armstrong, M. J. Sellars, and N. B. Manson, Infrared emission of the NV centre in diamond: Zeeman and uniaxial stress studies, *New J. Phys.* **10**, 103024 (2008).

[23] C. E. Carroll and F. T. Hioe, Three-state systems driven by resonant optical pulses of different shapes, *J. Opt. Soc. Am. B* **5**, 1335 (1988).

[24] Y. H. Issoufa and A. Messikh, Effect of dephasing on superadiabatic three-level quantum driving, *Phys. Rev. A* **90**, 055402 (2014).

[25] A. Shabani and H. Neven, Artificial quantum thermal bath: Engineering temperature for a many-body quantum system, *Phys. Rev. A* **94**, 052301 (2016).

[26] J. Zhang, J. H. Shim, I. Niemeyer, T. Taniguchi, T. Teraji, H. Abe, S. Onoda, T. Yamamoto, T. Ohshima, J. Isoya, and D. Suter, Experimental implementation of assisted quantum adiabatic passage in a single spin, *Phys. Rev. Lett.* **110**, 240501 (2013).

[27] A. Vepsäläinen, S. Danilin, and G. Sorin Paraoanu, Superadiabatic population transfer in a three-level superconducting circuit, *Science Advances* **5**, 5999 (2019).

[28] Y. X. Du, Z. T. Liang, Y. C. Li, X. X. Yue, Q. X. Lv, W. Huang, X. Chen, H. Yan, and S. L. Zhu, Experimental realization of stimulated Raman shortcut-to-adiabatic passage with cold atoms, *Nat. Commun.* **7**, 12479 (2016).

[29] J. Kölbl, A. Barfuss, M. S. Kasperczyk, L. Thiel, A. A. Clerk, H. Ribeiro, and P. Maletinsky, Initialization of single spin dressed states using shortcuts to adiabaticity, *Phys. Rev. Lett.* **122**, 090502 (2019).

[30] A. Barfuss, J. Teissier, E. Neu, A. Nunnenkamp, and P. Maletinsky, Strong mechanical driving of a single electron spin, *Nat. Phys.* **11**, 820 (2015).

- [31] J. Klatzow, J. N. Becker, P. M. Ledingham, C. Weinzel, K. T. Kaczmarek, D. J. Saunders, J. Nunn, I. A. Walmsley, R. Uzdin, and E. Poem, Experimental demonstration of quantum effects in the operation of microscopic heat engines, *Phys. Rev. Lett.* **122**, 110601 (2019).
- [32] J. P. Tetienne, L. Rondin, P. Spinicelli, M. Chipaux, T. Debuisschert, J. F. Roch, and V. Jacques, Magnetic-field-dependent photodynamics of single NV defects in diamond: an application to qualitative all-optical magnetic imaging, *New J. Phys.* **14**, 103033 (2012).
- [33] K. Funo, N. Shiraishi, and K. Saito, Speed limit for open quantum systems, *New J. Phys.* **21**, 013006 (2019).
- [34] P. Pietzonka and U. Seifert, Universal trade-off between power, efficiency, and constancy in steady-state heat engines, *Phys. Rev. Lett.* **120**, 190602 (2018).
- [35] M. G. Bason, M. Viteau, N. Malossi, P. Huillery, E. Arimondo, D. Ciampini, R. Fazio, V. Giovannetti, R. Mannella, and O. Morsch, High-fidelity quantum driving, *Nat. Phys.* **8**, 147 (2012).
- [36] H. Zhou, Y. Ji, X. Nie, X. Yang, X. Chen, J. Bian, and X. Peng, Experimental realization of shortcuts to adiabaticity in a nonintegrable spin chain by local counterdiabatic driving, *Phys. Rev. Applied* **13**, 044059 (2020).